MAHLER'S CONJECTURE IN CONVEX GEOMETRY: A SUMMARY AND FURTHER NUMERICAL ANALYSIS

A Thesis
Presented to
The Academic Faculty

by

Philipp Hupp

In Partial Fulfillment
of the Requirements for the Degree
Master of Science in the
School of Mathematics

Georgia Institute of Technology
December 2010

MAHLER'S CONJECTURE IN CONVEX GEOMETRY: A SUMMARY AND FURTHER NUMERICAL ANALYSIS

Approved by:

Professor Evans Harrell, Advisor
School of Mathematics
Georgia Institute of Technology

Professor Mohammad Ghomi
School of Mathematics
Georgia Institute of Technology

Professor Michael Loss
School of Mathematics
Georgia Institute of Technology

Date Approved: July 23, 2010

ACKNOWLEDGEMENTS

My deepest appreciation to my supervisor, Prof. Evans Harrell, for his encouragement and guidance during my studies. I feel fortunate to have him as my advisor. His original mind, his keen insight in approaching hard problems, and his vast knowledge have served as an inspiration for me throughout this thesis. I am particularly thankful to him for introducing me to the subjects of convex and differential geometry. He taught these subjects in an effortless manner and just that allowed me to accomplish this thesis.

A special thanks goes to Prof. Mohammad Ghomi for sharing his expertise on Mahler's conjecture with me and I would like to express my gratitude to him and Prof. Michael Loss as the members of my committee.

Furthermore I like to thank Michael Music who shared Prof. Harrell's working seminar with me. It was fun working with you Michael and all the best for your graduate studies.

TABLE OF CONTENTS

LIST OF TABLES

LIST OF FIGURES

SUMMARY

In this thesis we study Mahler's conjecture in convex geometry, give a short summary about its history, gather and explain different approaches that have been used to attack the conjecture, deduce formulas to calculate the Mahler volume and perform numerical analysis on it.

The conjecture states that the Mahler volume of any symmetric convex body, i.e. the product of the volume of the symmetric convex body and the volume of its dual body, is minimized by the (hyper-)cube. The conjecture was stated and solved in 1938 for the 2-dimensional case by Kurt Mahler. While the maximizer for this problem is known (it is the ball), the conjecture about the minimizer is still open for all dimensions greater than 2.

A lot of effort has benn made to solve this conjecture, and many different ways to attack the conjecture, from simple geometric attempts to ones using sophisticated results from functional analysis, have all been tried unsuccesfully. We will present and discuss the most important approaches.

Given the support function of the body, we will then introduce several formulas for the volume of the dual and the original body and hence for the Mahler volume. These formulas are tested for their effectiveness and used to perform numerical work on the conjecture. We examine the conjectured minimizers of the Mahler volume by approximating them in different ways. First the spherical harmonic expansion of their support functions is calculated and then the bodies are analyzed with respect to the length of that expansion. Afterwards the cube is further examined by approximating its principal radii of curvature functions, which involve Dirac δ functions.

CHAPTER I

INTRODUCTION

The Mahler volume, or volume product, first introduced by Kurt Mahler in 1939 [16], describes the volume of a convex body times the volume of its dual body. This thesis examines the Mahler volume in detail, gives the neccessary background in convex geometry to understand the functional, summarizes known results about the volume product, derives formulas to calculate it and performs numerical work using these formulas. The experiments focus on the open conjecture about the Mahler volume: Mahler suspected the cube to be one minimizer of the volume product in any dimension n [15]. So far this conjecture has only been proved for the 2 dimensional case by Mahler himself, just a few months after he stated the conjecture.

This work begins by introducing the volume product and the necesssary background in convex geometry. As we are looking at convex bodies, two useful ways to describe them, the support and the gauge function, are introduced. The volume product is closely related to duality, since its definition directly contains the dual body. So the relationship between the support function of a body and the gauge function of the dual body is emphasized. We further introduce the (generalized) Legendre transform and show how it links the support function of a body to its gauge function. Therefore we get a complete correlation between the gauge and support functions of a convex body and the support and gauge functions of the dual body. As we later want to approximate the conjectured minimizers of the Mahler volume, we will introduce metrics for the family of convex bodies. This allows to judge the quality of the approximation.

We continue with summarizing known results about the volume product. In contrast

to the lower bound, the upper bound of the Mahler volume is completely understood. The ball has been proved to be the maximizer of the volume product by Blaschke and Santaló [3, 4, 23]. Although we do not know if the cube minimizes the volume product, there are partial results on this conjecture. For certain families of convex bodies, the cube was succesfully proved to minimize the volume product. Asymptotic lower bounds on the Mahler volume are as well known and have been improved recently. Results about the structure of the minimizers are rare, and just one necessary condition about the boundary of the minimizers is known.

After the background of Mahler's conjecture is discussed, we derive formulas to calculate it given the support function of the body. We will often work in spherical coordinates, as the support and gauge function are homogeneous of degree 1 and hence allow us to make that restriction without loss of information. Formulas for the volume of the dual body are more straightforward to derive, if we have the support function in hand. So we begin with them. For the volume of the original body either the (generalized) Legendre transform, discussed earlier, can be used, or the principal radii of curvature play an important role in these formulas.

To test the performance of the just derived formulas, we carry out the numerical experiments. These experiments focus on 3 dimensions, as this is the easiest open case. After evaluating the different formulas, we approximate the conjectured minimizer in two different ways, to see, if a body of lower volume product can be generated like that. First, both conjectured minimizers, the cube and the cross polytope, are approximated by the spherical harmonic expansion of their support function. Although these bodies will be very close to the conjectured minimizers, their volume product stays within several percent of the conjectured value. Furthermore we determine that the approximations are not convex. The second approximation works on the principal radii of curvature of the cube. These functions are Dirac δ functions and we approximate them. Having the principal curvatures we can deduce the according support

function and hence have the body on hand.

We conclude the thesis by summarizing the experimental results giving future research ideas. In particular the numerical algorithms using the Legendre transform can be improved. Furthermore we give partial differential equations whose solution is the support function of the cube, when we approximate the Dirac δ functions in its radii of curvature by Gaussians. The numerical experiments suggest that the corresponding body may have a smaller volume product than the cube.

CHAPTER II

MAHLER'S CONJECTURE AND CONVEXITY

2.1 Mahler's Conjecture

Mahler's conjecture addresses convex bodies and their polar duals in $\mathbb{R}^n$. So before discussing the conjecture itself, we provide a brief review of the necessary definitions. A set $S \in \mathbb{R}^n$ is said to be convex if for all $x, y \in S$ and all $\lambda \in [0,1]$ the line between x and y, $\{z = \lambda x + (1-\lambda)y : \ x, y \in S, \ \lambda \in [0,1]\}$, is in S as well. The convex set is a convex body, if it is in addition compact, i.e. closed and bounded, and has non-empty interior. For this thesis $\mathbb{K}^n$ will denote the family of all convex bodies in $\mathbb{R}^n$. A set $S \in \mathbb{R}^n$ is said to be symmetric (with respect to the origin) if $-S = S$, i.e. if $x \in S \Rightarrow -x \in S$.

Given $K \in \mathbb{K}^n$ the polar dual or dual body K° of K is defined as

$$K^\circ = \{x \in \mathbb{R}^n : \ \langle x, y \rangle \leq 1 \ \forall \ y \in K\} \ . \tag{1}$$

Here $\langle \cdot, \cdot \rangle$ denotes the euclidean scalar product of $\mathbb{R}^n$.

Two easily verified facts about the polar body are: If K is a symmetric convex body in $\mathbb{R}^n$ then so is K°; and if K, L are convex bodies such that $K \subset L$, then $L^\circ \subset K^\circ$. Flats of the original body correspond to vertices of the dual body and vice versa. If the original body is scaled the dual body will scale by the inverse factor. Smooth areas of the original body correspond to smooth areas of the dual body and the dual of a ball of radius λ is the ball of radius $\frac{1}{\lambda}$.

The Minkowski sum of two sets $S, T \in \mathbb{R}^n$ is defined as $S + T := \{s + t \in \mathbb{R}^n : \ s \in S, \ t \in T\}$ and for $\lambda > 0$ we define similarly $\lambda \cdot S := \{\lambda s \in \mathbb{R}^n : \ s \in S\}$. It is now easily checked that the set of convex bodies $\mathbb{K}^n$ is a cone itself, i.e. it is closed under the Minkowski sum and under non-negative scalar multiplication.

With these definitions on hand we can introduce the Mahler volume and state the conjecture:

Definition 2.1.1 (Mahler volume):

Given a symmetric convex body $K \in \mathbb{K}^n$, its Mahler volume $M(K)$ is defined to be the quantity

$$M(K) := V_n(K)V_n(K^\circ) \,, \tag{2}$$

where $V_n(K)$ denotes the n-dimensional Lebesgue measure of K.

This definition yields several properties of the Mahler volume.

Proposition 2.1.2 (Basic properties of the Mahler volume [27]):

The Mahler volume $M(K)$ of a symmetric convex body $K \in \mathbb{K}^n$ has the following properties:

- Duality: $(K^\circ)^\circ = K$ implies that $M(K) = M(K^\circ)$.
- Affine invariance: If $T : \mathbb{R}^n \to \mathbb{R}^n$ is any invertible linear transformation, then $(TK)^\circ = (T^*)^{-1}K^\circ$ and hence $M(TK) = M(K)$.

Conjecture 2.1.3 (By Mahler 1939 [16]):

For a symmetric convex body $K \in \mathbb{K}^n$ the following inequalities hold

$$\frac{4^n}{n!} \leq M(K) \leq \frac{\pi^n}{\Gamma\left(\frac{n}{2}+1\right)^2} \,, \tag{3}$$

where $\Gamma(\cdot)$ denotes the Gamma Function, given by $\Gamma(x) = \int_0^\infty e^s x^{s-1}\, ds$ for $x > 0$. The lower bound is achieved by the dual pair of cube and cross-polytope and the upper bound by the ball.

Note that the dual body of the unit ball B^n is the unit ball itself, the cube in $\mathbb{R}^n$ is given by $I^n := \left\{(x_1, \ldots, x_n) \in \mathbb{R}^n : \ |x_i| \leq 1 \ \forall\ i \in \{1, \ldots, n\}\right\}$ and the cross-polytope by $O^n := \left\{(x_1, \ldots, x_n) \in \mathbb{R}^n : \sum_{i=1}^n |x_i| \leq 1\right\}$. In $\mathbb{R}^3$ the cross-polytope is often called

octahedron as well.

Since the Mahler volume is invariant under affine transformations, there are not just these extreme bodies but families consisting of all bodies that can be generated out of the specific ones by affine transformations. In fact, Mahler used the the general wording when he stated the extreme cases of the conjecture. He did not claim that these bodies are the unique extreme cases for the volume product. But it is now known that the ball and its affine transformations are the unique maximizers of it.

While checking that the given bodies take the conjectured lower and upper bounds is easy, proving the bounds is very difficult. The upper bound has been proved by Blaschke (for the 2-dimensional case) and Santaló (in full generality), and the result is known as Santaló's Inequality.

The lower bound is open except for the case when $n = 2$, which was proved by Mahler one month after he stated the conjecture [15]. We will discuss these results in more detail later when the history and results about the conjecture are reviewed.

Symmetry is not required for either the polar dual or the Mahler volume. If the symmetry constraint is dropped, it may instead be assumed that the origin is in the interior of the body, so that the dual body behaves nicely. Now the similar question, which convex bodies containing the origin in their interior minimize the Mahler volume, can be asked. In this case the conjectured minimum is the simplex.

2.2 Interpretation of Mahler's conjecture

Having the functional Mahler volume in hand it would be nice to have an intuition what it measures. There are two main approaches:

- **Volume Approach:** The Mahler volume functional indeed describes the volume of a specific body. Given a symmetric convex body $K \in \mathbb{K}^n$ we can look at $K \times K^\circ \in \mathbb{R}^n \times \mathbb{R}^n$. Then $M(K) = V_{2n}(K \times K^\circ)$.

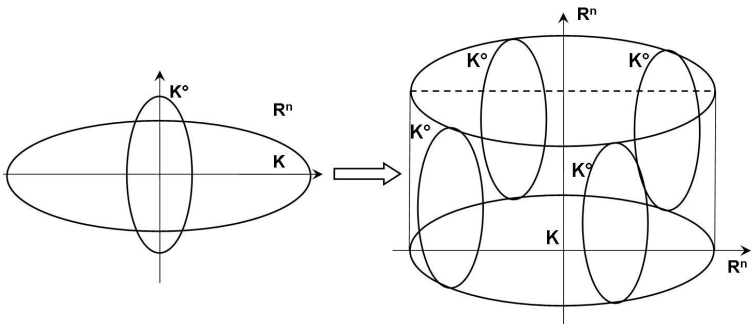

Figure 1: $K \times K^\circ$ as body in $\mathbb{R}^{2n}$

- **Pointedness Approach [26]:** Having the conjectured extreme cases of the Mahler volume in mind, the cube and the ball, one may think of the Mahler volume as capturing the "roundness" of a body. The ball is the roundest body one can think of and cubes and cross-polytopes are the pointiest symmetric ones. While we have a lot of tools and a good intuition to describe the ball as the roundest body, there is nothing comparable to say about the pointiness of a body. This is the weakness of this interpretation, since it does not make precise what it means for a body to be pointy.

While both approaches give a rough idea about what the Mahler volume is capturing, they do not provide a rigorous understanding of the functional.

2.3 The support and the gauge function of a convex set

For dealing with Mahler's conjecture we need to represent and describe convex bodies. In particular we are interested in a representation of the bodies that makes it easy to identify the body, get an intuition about how it looks, calculate metric quantities easily (in particular the volume of the body and its dual) and are able to modify it. In convexity two concepts have mainly proved useful for that: The support and the gauge functions of a convex body. Both concepts will be introduced now and shown

how they are related through the concept of duality and the Legendre transformation. Since all the concepts presented in this section are well known results in convexity the discussion will be brief. For an entire discussion including detailed proofs of all statements we refer to [28].

Definition 2.3.1 (Support and gauge function):

Given a convex body $K \in \mathbb{K}^n$ we define the support function $h_K(x)$ of K

$$h_K(x) = \sup\big\{ \langle x, k\rangle : \ k \in K\big\} \tag{4}$$

for $x \in \mathbb{R}^n$. If additionally the origin is an interior point of K we define

$$g_K(x) = \inf\big\{\lambda \geq 0 : \ x \in \lambda A\big\} \tag{5}$$

as its gauge function $g_K(x)$. The subscripts of the support and gauge function will be dropped when it is obvious to which body they refer to.

Both functions are well defined. Since K is non-empty and bounded so is $\big\{ \langle x, k\rangle : k \in K\big\}$ for any $x \in \mathbb{R}^n$, since the inner product is continuous. Furthermore the bilinearity of the inner product implies that this supremum does not change if we restrict the points k to be in the boundary of K.

$$h(x) = \sup\big\{ \langle x, k\rangle : \ k \in K\big\} = \sup\big\{ \langle x, k\rangle : \ k \in \partial K\big\}\ , \tag{6}$$

where ∂K denotes the boundary of K. In the case of the gauge function, the origin being an the interior of K ensures that we can find an open ball $B_\epsilon(0)$ centered at the origin that is inside K. Then $x \in \big(\frac{||x||}{\epsilon} + 1\big)B_\epsilon(0) \subset \big(\frac{||x||}{\epsilon} + 1\big)K$, and so g takes finite values for any $x \in \mathbb{R}^n$.

For an intuition about the support function consider any $u \in \mathbb{R}^n\backslash\{0\}$ and any $\alpha \in \mathbb{R}$ and look at the hyperplane with normal u that is given by $H_\alpha = \big\{x \in \mathbb{R}^n : \langle u, x\rangle = \alpha\big\}$ and at the half space defined by $H_\alpha^- = \big\{x \in \mathbb{R}^n : \langle u, x\rangle \leq \alpha\big\}$. Different α result in a family of hyperplanes that are all parallel. For any closed convex body K there will

be two cases where H_α supports K. But in only one of these cases it is additionally true that $K \subset H_\alpha^-$. Obviously we have $K \subset H_\alpha^-$ if and only if $\langle u, k\rangle \leq \alpha \quad \forall\, k \in K$, i.e. if and only if

$$\sup\big\{\, \langle u, k\rangle :\ k \in K\big\} \leq \alpha\ .$$

If we also require that H_α supports K, we need some point $k_0 \in K$ s.t. $\langle u, k_0\rangle = \alpha$. This yields that H_α is the support hyperplane according to the normal u such that $K \subset H_\alpha^-$ if and only if

$$\sup\big\{\, \langle u, k\rangle :\ k \in K\big\} = \alpha\ .$$

Furthermore, if u is a unit vector, i.e. if $||u|| = 1$, then $h(u)$ gives the distance to the origin of the support hyperplane with normal u such that $K \subset H_\alpha^-$.

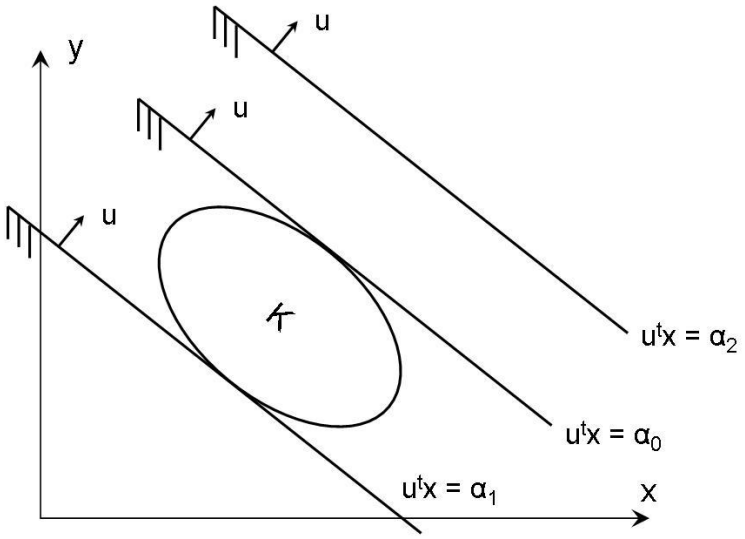

Figure 2: Supporting hyperplanes for a convex body

For an intuition about the gauge function consider the set

$$S = \big\{x \in \mathbb{R}^n :\ g(x) \leq 1\big\}\ .$$

It is clear that $x \in K \Rightarrow g(x) \leq 1$ and $x \notin K \Rightarrow g(x) > 1$. So K can be thought of as the level set S of g at the value 1. Additionally $\{x \in \mathbb{R}^n : \ g(x) = 1\}$ describes the boundary of K. Let us embed K in $\mathbb{R}^{n+1}$ by $K \times \{1\}$ and take the convex hull of $K \times \{1\}$ and the origin. If we then intersect this construction with a hyperplanes with normal $(\overbrace{0, \ldots, 0}^{n \text{ 0's}}, 1)$ and distance $0 \leq \alpha \leq 1$ from the origin we gain copies of K scaled by α given by $\{x \in \mathbb{R}^n : \ g(x) \leq \alpha\}$.

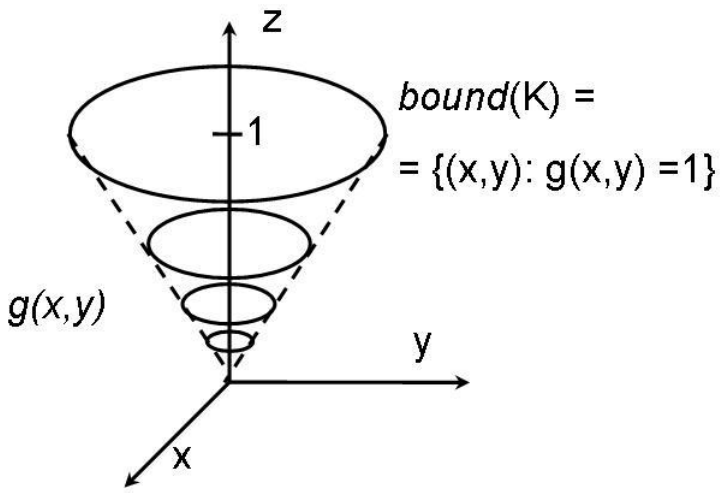

Figure 3: The gauge function of a convex set K

We will call a convex body $K \in \mathbb{K}^n$ smooth, if every point x on its boundary has a unique support plane, i.e. if it has a unique outward normal u [24].

Definition 2.3.2 (Convex and positive homogeneous functions and the epigraph of f):

A function $f : X \to \mathbb{R}$ defined on a non-empty convex set $X \subset \mathbb{R}^n$ is said to be convex if

$$f\big(\lambda x + (1-\lambda)y\big) \leq \lambda f(x) + (1-\lambda) f(y) \qquad \forall\, x, y \in X \text{ and } \forall\, \lambda \in [0,1]\,. \quad (7)$$

The convexity of X ensures that $\lambda x + (1-\lambda)y$ is always in X as well.

Associated with any function $f : X \to \mathbb{R}$ defined on a non-empty compact set X is a subset of $\mathbb{R}^{n+1}$, its epigraph,

$$\left\{(x_1, \ldots, x_n, x) : \ (x_1, \ldots, x_n) \in X, \ x \geq f(x_1, \ldots, x_n)\right\} . \tag{8}$$

It is easily checked that f is convex if and only if its epigraph is a convex subset of $\mathbb{R}^{n+1}$.

A function $f : C \to \mathbb{R}$ defined on a convex cone $C \subset \mathbb{R}^n$ is said to be positively homogeneous if

$$f(\lambda x) = \lambda f(x) \qquad \forall\ x \in C \text{ and } \forall\ \lambda \geq 0 . \tag{9}$$

Theorem 2.3.3 (Properties of the support function):

The support function h of any convex body $K \in \mathbb{K}^n$ is positively homogeneous and convex. Furthermore any positively homogeneous and convex function h gives rise to a convex body $K \in \mathbb{K}^n$ defined by

$$K = \left\{x \in \mathbb{R}^n : \langle u, x\rangle \leq h(u)\ \forall\ u \in \mathbb{R}^n\right\} . \tag{10}$$

When K is given by (10) it has support function h.

The theorem states that there is a bijection between the positively homogeneous, convex functions and the convex bodies. A similar result is true for the gauge function.

Theorem 2.3.4 (Properties of the gauge function):

The gauge function g of closed convex set $K \in \mathbb{K}^n$ that contains the origin in its interior is non-negative, positively homogeneous and convex. Furthermore any non-negative, positively homogeneous and convex function $g(x)$ gives rise to a convex body $K \in \mathbb{K}^n$ defined by

$$K = \left\{x \in \mathbb{R}^n : \ g(x) \leq 1\right\} . \tag{11}$$

When K is given by (11) it has gauge function $g(x)$ and it is obvious that the origin is an interior point of K.

If a function $f : \mathbb{R}^n \to \mathbb{R}$ is positively homogeneous it may simply be regarded as a function of the unit sphere $S^{n-1} = \left\{x \in \mathbb{R}^n : \ ||x|| = 1\right\}$ without loss of any information. If $f : S^{n-1} \to \mathbb{R}$ is defined, then it is easily extended to all $x \in \mathbb{R}^n$ by $f(x) = f\left(x\frac{||x||}{||x||}\right) = ||x||f\left(\frac{x}{||x||}\right)$. Hence we will often refer to the support and gauge function as defined on the unit sphere.

It is well known that convex functions have nice properties and so have the support and gauge function of convex sets. We will use that convex functions defined on a set X are continuous on X. Furthermore a convex function possesses all its one sided partial derivatives for any point x in the interior of X.

Theorem 2.3.5 (Support and gauge function and the dual body):

Let h be the support and g be the the gauge function of a convex body $K \in \mathbb{K}^n$ that has the origin as an interior point. Then the support and the gauge function of the dual body K° are g and h respectively.

Proof. If $u \in K^\circ$ then $\langle u, k\rangle \leq 1 \quad \forall \ k \in K$ this means $h(u) \leq 1$. Conversly if $h(u) \leq 1$ then $\langle u, k\rangle \leq 1$ and so $u \in K^\circ$. So we have

$$K^\circ = \left\{u \in \mathbb{R}^n : \ h(u) \leq 1\right\}.$$

Since the origin is an interior point of K, the support function h is non-negative. Therefore h is a non-negative, positively homogeneous, convex function such that equation (11) holds. Hence h is the support function of K°. From this we can also conclude that the support function of K° is the gauge function of K. □

To illustrate the above concepts we will discuss some examples of convex bodies and will calculate their support and gauge functions explicitly.

Example 2.3.6 (The support and gauge function of the ball):

Given the ball with radius $\lambda > 0$ centered at the origin $B_\lambda(0)$, we first determine

its support function. Therefore consider any $u \in S^{n-1}$. Both support planes with normal u have distance λ from the origin for any $u \in S^{n-1}$. So $h \equiv \lambda$. Since

$$B_\lambda(0)^\circ = B_{\frac{1}{\lambda}}(0)$$

the gauge function is $g \equiv \frac{1}{\lambda}$ as the support function of the dual body.

Example 2.3.7 (The support and gauge functions of the cube and the cross-polytope):

Recall the definitions for the cube I^n and the cross-polytope O^n

$$I^n = \left\{(x_1, \ldots, x_n) \in \mathbb{R}^n : \ |x_i| \leq 1 \ \forall \ i \in \{1, \ldots, n\}\right\}, \tag{12}$$

$$O^n = \left\{(x_1, \ldots, x_n) \in \mathbb{R}^n : \sum_{i=1}^{n} |x_i| \leq 1\right\}, \tag{13}$$

respectively. We first determine the support function of the cube. Again consider any $u \in S^{n-1}$ and look at the support plane with normal u such that I^n is in the negative half-space corresponding to that hyperplane. The support hyperplane has to touch I^n at at least one point. Now recall that given a point x_0 in the hyperplane and the normal vector of the hyperplane u it can be represented by

$$\left\{x \in \mathbb{R}^n : \ \langle u, x\rangle = \langle u, x_0\rangle\right\}, \tag{14}$$

and if u has norm one the distance of that hyperplane from the origin is given by $\langle u, x_0\rangle$. Going back to the cube we see that at least one of the points of contact has to be one of the vertices of the cube. These vertices are given by $\big(\overbrace{\pm 1, \ldots, \pm 1}^{n \text{ times}}\big)$. At which of these vertices does the plane support the cube? It is the vertex of the orthant[1] in which the normal is pointing (if there are several, i.e. the normal is parallel to at least one of the coordinate axis, we just choose any of the appropriate

[1]Orthant is the generalization of quadrant (in 2 dimensions) and octant (in 3 dimensions) to arbitrary dimensions.

vertices). So the vertex has the same sign as the normal vector for each coordinate. Hence the support function of the cube is given by

$$h_{I^n}(u) = \sum_{i=1}^{n} |u_i| \ . \tag{15}$$

Similarly, we get the support function of the cross-polytope. The vertices of the cross-polytope are given by $\big(\overbrace{0,\dots 0}^{k \text{ times}}, \pm 1, \ \overbrace{0,\dots,0}^{n-k-1 \text{ times}}\ \big)$ for $0 \leq k \leq n-1$. So just one coordinate of the normal will determine the support function. The vertex the plane supports the cross-polytope at has to be the vertex for which $|u_i|$ takes its largest value. Since again u points in the direction of that vertex the signs of the according coordinates are the same and the support function is given by

$$h_{O^n}(u) = \max_{1 \leq i \leq n} |u_i| \ . \tag{16}$$

Using Theorem 2.3.5 we also know the gauge functions of both bodies. Observe that equations (15) and (16) are just the l^1 and l^∞ norms of the normal vector u for the cube and the cross-polytope respectively.

Example 2.3.8 (The support function of the cylinder):

Let us look at a cylinder whose rotation axis is the x_3-axis of the coordinate system. Let its total height be 2 and the radius of its base be 1. When we evaluate the support function at (x, y, z) we need the coordinates of the point where this vector supports the body. For $z > 0$ the contact point will be at the upper base, for $z < 0$ at the lower base, and for $z = 0$ in the x_1x_2-plane. The exact point of contact is further determined by the x and y coordinates of the vector. It will be at the unit direction corresponding to x and y, and hence the support point is

$$\begin{pmatrix} \frac{x}{\sqrt{x^2+y^2}} \\ \frac{y}{\sqrt{x^2+y^2}} \\ sgn(z) \end{pmatrix} ,$$

where

$$sgn(x) = \begin{cases} 1, & \text{for } x > 0, \\ 0, & \text{for } x = 0, \\ -1, & \text{for } x < 0 \end{cases}$$

denotes the signum function. Hence the value of the support function, given by the inner product of the normal with the corresponding support point, is

$$h(x,y,z) = \left\langle \begin{pmatrix} x \\ y \\ z \end{pmatrix}, \begin{pmatrix} \frac{x}{\sqrt{x^2+y^2}} \\ \frac{y}{\sqrt{x^2+y^2}} \\ sgn(z) \end{pmatrix} \right\rangle = \sqrt{x^2+y^2} + |z| \, . \tag{17}$$

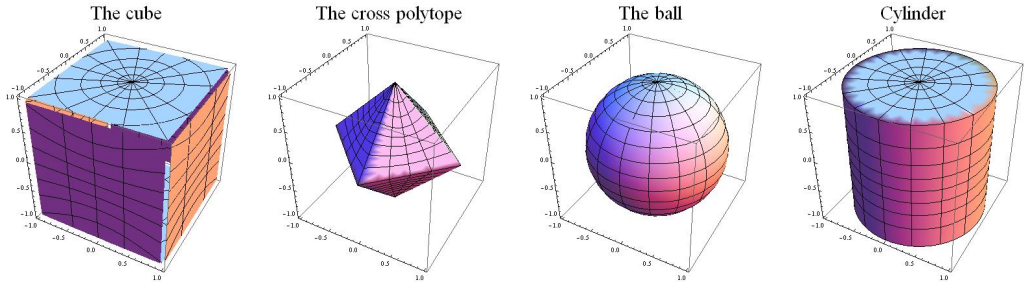

Figure 4: The cube, the cross polytope, the ball and the cylinder in $\mathbb{R}^3$

Theorem 2.3.9 (The Minkowski sum and the support function):

For $K, L \in \mathbb{K}^n$ and $\lambda > 0$ it is true that

$$h_{K+L} \equiv h_K + h_L \quad \text{and} \tag{18}$$

$$h_{\lambda K} \equiv \lambda h_K \, . \tag{19}$$

Proof. Consider any $x \in S^{n-1}$. We then have

$$h_{K+L}(x) = \sup\left\{\langle x, k+l\rangle : \; k+l \in K+L\right\} = \sup\left\{\langle x,k\rangle + \langle x,l\rangle : \; k \in K, \; l \in L\right\} =$$

$$= \sup\left\{\langle x,k\rangle : \; k \in K\right\} + \sup\left\{\langle x,l\rangle : \; l \in L\right\} = h_K(x) + h_L(x) \, .$$

Analogously it is true that

$$h_{\lambda K}(x) = \sup\left\{\langle x, \lambda k\rangle : \ \lambda k \in \lambda K\right\} = \sup\left\{\lambda\langle x, k\rangle : \ k \in K\right\} = \\ = \lambda \sup\left\{\langle x, k\rangle : \ k \in K\right\} = \lambda h_K(x) \ .$$

□

Beside the nice aspect that the support and gauge function of a body coincide with the gauge and support function of the dual body respectively, there is another relation between these functions involving the Legendre transformation. Before we introduce this concept, let us discuss how convex bodies can be said to distinct from or close to another.

2.4 The Hausdorff and the L^2 distace for the set of convex bodies

To examine Mahler's conjecture we want to build bodies that are similar, in some sense, to the conjectured minimizers. For the family of sets in $\mathbb{R}^n$ the most common distance function is the Hausdorff distance. For the set of convex bodies with the origin in the interior this concept can be extended to lead to all L^p distances. Our discussion of the different metrics in this chapter follows the corresponding chapter in [9].

First let us introduce the parallel body. Having a convex body $K \in \mathbb{K}^n$ and some $r \geq 0$ the parallel body of K at distance r is defined to be

$$K_{(r)} = K + r \cdot B^n \ , \tag{20}$$

and is another convex body. From Theorem 2.3.9 about the Minkowski sum and support function we get $h_{K_{(r)}} = h_K + r$. For smooth parts of the body K the parallel body can as well be constructed by flowing each boundary point outward in its normal direction at a constant rate.

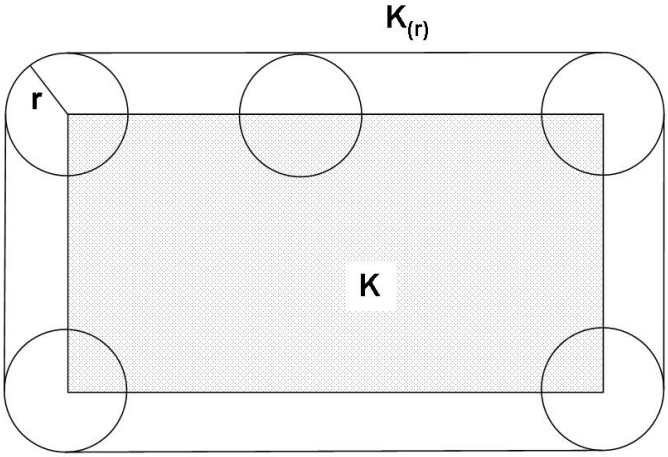

Figure 5: The parallel body $K_{(r)}$ of the rectangle K

Definition 2.4.1 (The Hausdorff distance):

For any $K, L \in \mathbb{K}^n$ the Hausdorff distance $\delta(K, L)$ of K and L is defined as

$$\delta(K, L) = \inf\{r : \ K \subset L_{(r)}, \ L \subset K_{(r)}\} \ . \tag{21}$$

Since K and L are bounded this infimum is always finite. We can also rewrite the definition of the Hausdorff distance in terms of the support function and get

$$\delta(K, L) = \sup\{|h_K(\omega) - h_l(\omega)| : \ \omega \in S^{n-1}\} \ . \tag{22}$$

Looking at the Banach space of continuous functions over S^{n-1} this equation becomes

$$\delta(K, L) = ||h_K - h_L||_\infty \ . \tag{23}$$

With that formula it is easily checked that the Hausdorff distance is a well defined metric since all properties follow immediately from the corresponding facts about the metric $||\cdot||_\infty$. While the Hausdorff distance gives a good intuition about closeness of two bodies, using the parallel body, other distances are sometimes easier to deal with. Similar to equation (23) we can use the L^p metrics for $p \geq 1$ on the space of square integrable functions over S^{n-1} to get metrics for the set of convex bodies, namely

$$\delta_p(K, L) = ||h_K - h_L||_p \ . \tag{24}$$

In particular the L^2 distance

$$\delta_2(K,L) = ||h_K - h_L||_2 = \Big(\int_{S^{n-1}} \big(h_K(\omega) - h_L(\omega)\big)^2 \, d\omega \Big)^{1/2} \tag{25}$$

is often used as it captures the same structure as the underlying Banach space. It can be shown, using regularity properties of convex functions, that the L^2 and the Hausdorff distance, which should be called L^∞ in this context, generate the same topology for the set of convex bodies.

2.5 The (generalized) Legendre transformation and duality

The Legendre transformation is a tool classically used in thermodynamics and mechanics, and for solving partial differential equations. Here we will link it to convexity and duality generalizing a proof given in [7]. The discussion of this transform in the literature is rather brief. References can be found in [21], [7], and [2]. For our discussion we will choose an approach similar to [6] and require that the function of interest is convex and superlinear.

Definition 2.5.1 (Superlinearity):

A convex function $f : \mathbb{R}^n \to \mathbb{R}$ is said to be superlinear if

$$\lim_{||x|| \to \infty} \frac{f(x)}{||x||} = +\infty \tag{26}$$

Definition 2.5.2 (The Legendre transformation):

Given a function $f : \mathbb{R}^n \to \mathbb{R}$ the Legendre transform $\mathcal{L}$ of f at a point $y \in \mathbb{R}^n$ is defined by

$$\mathcal{L}[f](y) = \sup_{x \in \mathbb{R}^n} \big\{ \langle y, x \rangle - f(x) \big\} \, . \tag{27}$$

If the function to which we apply the Legendre transform is convex and superlinear we know that the supremum is in fact taken for some x_0. Convexity of f ensures continuity of $\langle y, \cdot \rangle - f(\cdot)$ for all y and superlinearity implies that the maximum of $\langle y, \cdot \rangle - f(\cdot)$ is finite for all y.

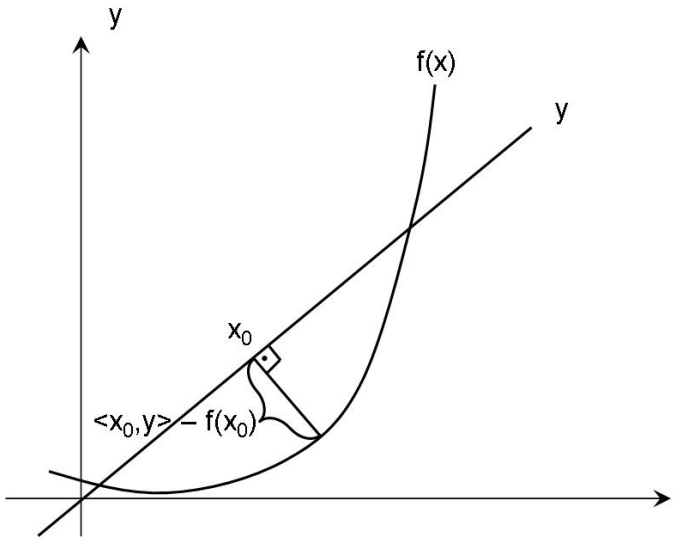

Figure 6: Calculating the Legendre Transform $\mathcal{L}[f](y)$

We can as well view $\langle y, x\rangle - f(x)$ as a function of x given a particular y. If we require that f is differentiable, we get the following necessary condition for an x_0 that maximizes this expression.

$$df(x_0) = y \ .$$

When we apply the Legendre transform to the support or the gauge function we do not have the properties required above, since none of these functions is superlinear. But if a function is positive and positively homogeneous of degree one, then its square is superlinear:

$$\frac{f(x)^2}{||x||} = \frac{f(||x||x_0)^2}{||x||} = \frac{||x||^2 f(x_0)^2}{||x||} = ||x|| f(x_0)^2 \to \infty \text{ for } ||x|| \to \infty \ ,$$

where $x_0 = \frac{x}{||x||}$. This discussion prepares the generalized Legendre transformation as introduced in [7]. For a function $f : \mathbb{R}^n \to \mathbb{R}$ such that f is positive, convex and positively homogeneous of degree one, the generalized Legendre transform of f is given by

$$\mathcal{L}\Big[\frac{f^2}{2}\Big](y) = \sup_{x \in \mathbb{R}^n} \Big\{ \langle y, x\rangle - \frac{f(x)^2}{2} \Big\} \ . \tag{28}$$

The supremum in equation (28) is always attained for some point $x_y \in \mathbb{R}^n$.

The following result that connects the Legendre transform to the principle of duality first appears in [7] with unnecessary conditions on the smoothness of the function of interest. Harrell generalized it to hold for support and gauge functions of arbitrary convex bodies and the proof was first published in [29] with reference to his work.

Theorem 2.5.3 (The generalized Legendre transform and duality):
Given a convex body $K \in \mathbb{K}^n$ that contains the origin in its interior, we denote by h and g its support and gauge functions, respectively. Then the following equality holds:

$$\mathcal{L}\Big[\frac{g^2}{2}\Big] = \frac{h^2}{2} \ . \tag{29}$$

Proof. We begin with showing $\mathcal{L}\Big[\frac{g^2}{2}\Big] \geq \frac{h^2}{2}$. First give any $y \in \mathbb{R}^n$. The convexity of g ensures its continuity and so $\{x \in \mathbb{R}^n : g(x) = 1\} = \partial K$ is a compact set. Hence there has to be some $x_0 \in \partial K$, i.e. $g(x_0) = 1$, such that

$$h(y) = \sup_{x \in \partial K} \big\{\langle y, x\rangle\big\} = \langle y, x_0\rangle \ .$$

Hence for any $\lambda > 0$,

$$\mathcal{L}\Big[\frac{g^2}{2}\Big](y) = \sup_{x \in \mathbb{R}^n}\{\langle y, x\rangle - \frac{g(x)^2}{2}\} \geq \langle y, \lambda x_0\rangle - \frac{g(\lambda x_0)^2}{2} = \\ = \lambda\langle y, x_0\rangle - \frac{\lambda^2}{2} g(x_0) = \lambda h(y) - \frac{\lambda^2}{2} \ .$$

Setting $\lambda = h(y)$, this yields

$$\mathcal{L}\Big[\frac{g^2}{2}\Big](y) \geq \lambda h(y) - \frac{h(y)^2}{2} = \frac{h(y)^2}{2} \ .$$

Let us now prove the reverse inequality, $\mathcal{L}\Big[\frac{g^2}{2}\Big] \leq \frac{f^2}{2}$. Again we consider an arbitrary $y \in \mathbb{R}^n$. The convexity and positive homogeneity of g ensure that we can find a x_0 such that

$$\mathcal{L}\Big[\frac{g^2}{2}\Big](y) = \sup_{x \in \mathbb{R}^n}\Big\{\langle y, x\rangle - \frac{g(x)^2}{2}\Big\} = \langle y, x_0\rangle - \frac{g(x_0)^2}{2}$$

We distinguish between two cases: If $g(x_0) = 0$ this implies $x_0 = 0$, since K is a bounded set. But $x_0 = 0$ would yield $\mathcal{L}\Big[\frac{g^2}{2}\Big](y) = 0 \leq \frac{h(y)^2}{2}$, since the origin is in the interior of K, and the proof is finished. Therefore assume that $g(x_0) \neq 0$. Consider the function p of one real variable defined by

$$p(\lambda) = \langle y, \lambda x_0 \rangle - \frac{g(\lambda x_0)^2}{2} = \lambda \langle y, x_0 \rangle - \lambda^2 \frac{g(x_0)^2}{2} \; .$$

This quadratic function in λ obviously takes its maximum for $\lambda_0 = \frac{\langle y, x_0 \rangle}{g(x_0)^2}$. This expression is well defined since we excluded the case $g(x_0) = 0$, and furthermore from $g(x_0) \neq 0$ and $\langle y, x_0 \rangle - \frac{g(x_0)^2}{2} = \sup_{x \in \mathbb{R}^n} \{\langle y, x \rangle - \frac{g(x)^2}{2}\} \geq \langle y, 0 \rangle - \frac{g(0)^2}{2} = 0$, we can conclude that

$$\langle y, x_0 \rangle \geq \frac{g(x_0)^2}{2} \geq 0 \; .$$

Hence we can deduce that $\lambda_0 \geq 0$, and finally get

$$\begin{aligned} \mathcal{L}\Big[\frac{g^2}{2}\Big](y) &= \langle y, 1 \cdot x_0 \rangle - \frac{g(1 \cdot x_0)^2}{2} \leq \langle y, \lambda_0 x_0 \rangle - \frac{g(\lambda_0 x_0)^2}{2} = \\ &= \lambda_0 \langle y, x_0 \rangle - \frac{\lambda_0^2 g(x_0)^2}{2} = \frac{\langle y, x_0 \rangle}{g(x_0)^2} \langle y, x_0 \rangle - \frac{\langle y, x_0 \rangle^2}{g(x_0)^4} \frac{g(x_0)^2}{2} = \\ &= \frac{\langle y, x_0 \rangle^2}{2 g(x_0)^2} = \frac{1}{2} \Big\langle y, \frac{x_0}{g(x_0)} \Big\rangle^2 \; . \end{aligned}$$

The observation that $g\big(\frac{x_0}{g(x_0)}\big) = 1$ yields that $\frac{x_0}{g(x_0)} \in \partial K$, and hence

$$\mathcal{L}\Big[\frac{g^2}{2}\Big](y) \leq \frac{1}{2} \Big\langle y, \frac{x_0}{g(x_0)} \Big\rangle^2 \leq \frac{1}{2} \sup_{x \in \partial K} \langle y, x \rangle^2 = \frac{h(y)^2}{2} \; .$$

The last inequality finishes the proof. □

Let us emphasize that Equation (29) does not relate only the support and gauge function of a convex body via the generalized Legendre Transform. Combining the Theorems 2.5.3 and 2.3.5, the support and gauge function of the body and its dual are all related. Given a convex body $K \in \mathbb{K}^n$ that contains the origin in its interior, let us denote with h, g its support and gauge function, K° its dual body, and with h°, g° the support and gauge function of the dual body, respectively. We then get

$$\mathcal{L}\Big[\frac{h^2}{2}\Big] = \mathcal{L}\Big[\frac{\big(g^\circ\big)^2}{2}\Big] = \frac{\big(h^\circ\big)^2}{2} = \frac{g^2}{2} \; . \tag{30}$$

This yields that the generalized Legendre transform is an involution for the set of support and gauge functions of convex bodies that contain the origin in their interior. So knowing one of the functions h, g, h° and g° we know all others. This relationship is summarized in figure 7.

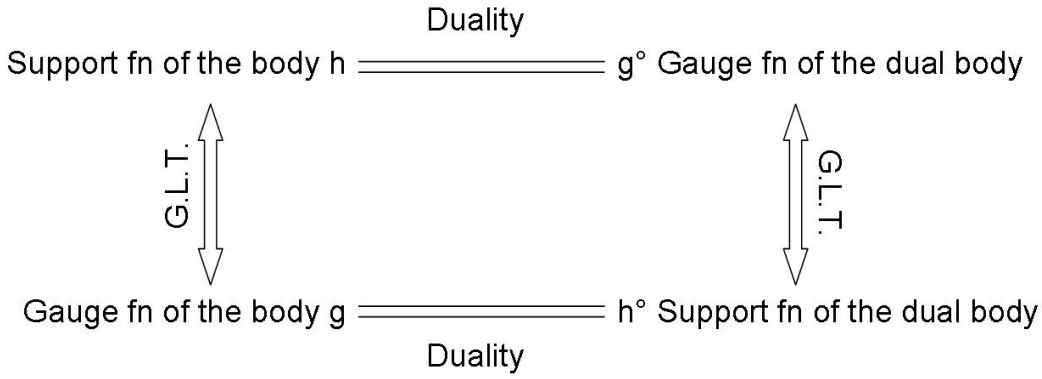

Figure 7: The generalized Legendre transform relates the original and dual support and gauge functions

CHAPTER III

KNOWN RESULTS ON MAHLER'S CONJECTURE

While the upper bound for the Mahler volume has been proved and is known as the Blaschke-Santaló inquality, the lower bound is still open. Nevertheless there are partial results on the lower bound, which can be categorized into three classes.

- **Lower bounds** for the Mahler volume have been proved with factors depending on the dimension n.
- For certain **families of convex bodies** Mahler's conjecture has been proved successfully.
- Some **necessary conditions** for the minimizer of the Mahler volume are known.

The most important results on the Mahler volume for symmetric convex bodies are presented in table (1) and will be discussed in this chapter.

3.1 The Blaschke Santaló Inequality

The upper bound for the Mahler volume is known to be

$$M(K) \leq \frac{\pi^{\frac{n}{2}}}{\Gamma\left(\frac{n}{2}+1\right)} = M(B^n) \quad \forall K \in \mathbb{K}^n \,, \tag{31}$$

and has been proved by Blaschke for the 3 dimensional case [4] and in generality by Santaló [23]. Under certain smoothness assumptions on the convex body the latter also includes equality statements for the above bound. It has been proved by Saint-Raymond [22] without further restrictions on the symmetric convex body that equality in (31) is obtained only for ellipsoids. These results are commonly known as the Blaschke Santaló Inequality.

Table 1: Known results on Mahler's Conjecture

Result	By	Year	Reference
Upper bounds			
$M(B^n) \quad \forall K \in \mathbb{K}^3$	Blaschke	1917, 1923	[3],[4]
$M(B^n) \quad \forall K \in \mathbb{K}^n \quad \forall n \in \mathbb{N}$	Santaló	1949	[23]
equality above only for ellipsoids	Saint-Raymond	1980	[22]
Lower bounds			
$\frac{4^2}{\Gamma(2+1)}$ for all polygons in $\mathbb{R}^2$	Mahler	1939	[15]
$c^n M(B^n)$ for some constant $c > 0$	Bourgain, Milman	1987	[5]
$\left(\frac{\pi}{4}\right)^{n-1} \frac{4^n}{\Gamma(n+1)} \quad \forall K \in \mathbb{K}^n \quad \forall n \in \mathbb{N}$	Kupperberg	2006	[13]
Families of bodies			
unit balls of $\mathbb{R}^n$ with 1-unconditional basis	Saint-Raymond	1980	[22]
Zonoids	Reisner	1985	[18]
Necessary conditions			
boundary of body cannot be of class C^2_+	Stancu	2009	[25]

A quite simple proof for it using Steiner symmetrizations is presented by Tao [27] and will be sketched here.

Sketch of the proof for the Blaschke-Santaló inequality. Given a set $K \in \mathbb{R}^n$, we define the Steiner symmetrization $S_0(K)$ of K with respect to 0 to be the set

$$S_0(K) := \frac{1}{2} \cdot (K - K) = \left\{ \frac{x-y}{2} : x, y \in K \right\} . \tag{32}$$

In general, if $\pi : \mathbb{R}^n \to \mathbb{R}^n$ is any orthogonal projection to a subspace of $\mathbb{R}^n$, the Steiner symmetral $S_\pi(K)$ of K with respect to π is defined to be the set

$$S_\pi(K) := \bigcup_{z \in \pi(K)} z + S_0(K \cap \pi^{-1}(z)) = \left\{ \frac{x-y}{2} + z : x, y \in K; z = \pi(x) = \pi(y) \right\} . \tag{33}$$

The inradius $r(K) > 0$ and circumradius $R(K) > 0$ of a convex body are defined to be the biggest and respectively lowest quantities such that

$$r(K) \cdot B^n \subset K \subset R(K) \cdot B^n , \tag{34}$$

and the eccentricity of K is defined as

$$e(K) := \frac{R(K)}{r(K)} \ . \tag{35}$$

The only body with eccentricity 1 is obviously the ball. It can be shown that Steiner symmetrizations do not increase the eccentricity of a convex body, while they also do not decrease the Mahler volume. Given the inclusion (34) and the monotonocity when taking the polar body we see that

$$e(K)^{-n} \cdot M(B^n) \leq M(K) \leq e(K)^n \cdot M(B^n) \ . \tag{36}$$

Hence it suffices to show that for any given convex body we can find a series of Steiner symmetrizations $K_0 = K,\ K_1 = S_{\pi_1}(K_0),\ K_2 = S_{\pi_2}(K_1),\ \ldots$, such that the eccentricity of the convex bodies converges to 1. This can be done in several ways; see for example [27] and [10]. □

The proof uses that the maximizer of the Mahler volume is uniquely the ball (up to affine transformations), and that we can transform every convex body into a ball with a sequence of Steiner symmetrizations. Giving a similar argument for the minimizer of the Mahler volume is very difficult, since the structure of the conjectured minimizing shapes is more complex. In higher dimensions there are shapes that are not affine transformations of the cube but apparently also minimize the Mahler volume [22]. Nevertheless similar approaches, i.e. given a convex body we modify it nicely so that it satisfies the properties we wish, have been used to obtain weaker lower bounds and necessary conditions on the boundary of a convex body.

3.2 Lower bounds for the Mahler volume

Lower bounds for the Mahler volume have been continuously improved in history and we give here a broader review as sketched in Table (1). One of the first bounds was obtained using John's theorem [11]. The theorem states that every symmetric convex

body $K \in \mathbb{K}^n$ contains a unique ellipsoid E of maximal volume. John furthermore proves that

$$E \subset K \subset \sqrt{n}E \tag{37}$$

if K is symmetric. Since we can tansform every ellipsoid into a ball with an invertible affine transformation and the Mahler volume does not change under these transformations, we can assume without loss of generality that the eccentricity of any given symmetric convex body is less or equal to $\sqrt{n}$. Combining this with equation (36) yields the simple bounds

$$n^{-\frac{n}{2}} M(B^n) \leq M(K) \leq n^{\frac{n}{2}} M(B^n) \; . \tag{38}$$

In [12] Kuperberg proves that

$$M(K) \geq \frac{M(B^n)}{(\log_2 n)^n} = \frac{\pi^{\frac{n}{2}} \Gamma(n+1)}{(\log_2 n)^n \Gamma(\frac{n}{2}+1) 4^n} \frac{4^n}{\Gamma(n+1)} \tag{39}$$

for every symmetric convex body $K \in \mathbb{K}^n$. This proof of Kuperberg uses mainly geometric arguments and a procedure to create a series of convex bodies. Roughly speaking, the proof follows an idea similar to the proof of the Blaschke-Santaló inequality with Steiner symmetrizations.

Bourgain and Milman [5] proved that there exists a constant $c > 0$ independent of n such that

$$M(K) \geq c^n M(B^n) \quad \forall \, n \in \mathbb{N} \; . \tag{40}$$

Although the proof constructs the constant $c > 0$ explicitly, no good value for it is known. The proof is involved and uses some strong results from functional analysis. The last and best result until now is again due to Kuperberg [13]. Kuperberg provides the constant $c = \frac{1}{2}$ for equality (40) using a different approach to the problem. His final result is

$$M(K) \geq \left(\frac{\pi}{4}\right)^{n-1} \frac{4^n}{\Gamma(n+1)} \tag{41}$$

for any symmetric convex body $K \in \mathbb{K}^n$. For his analysis he connects the Mahler volume to the bottleneck conjecture. The bottleneck conjecture deals with a set $K^\diamond \subset K \times K^\circ$ and states that the $K^\diamond$ is minimized over the set of centrally symmetric convex bodies when K is an ellipsoid. For the definition of $K^\diamond$ we need the subsets $K^\pm = \big\{(x,y) \in K \times K^\circ : \ x \cdot y = \pm 1\big\}$. The geometric join $A * B$ of two sets $A, B \in \mathbb{R}^n$ is defined as the union of all line segments that connect a point in A and a point in B. If $M \subset \mathbb{R}^n$ is a closed manifold of codimension 1, the filling $\overline{M}$ of M is the compact region in $\mathbb{R}^n$ that is enclosed by M. If $A * B$ is such a manifold, we call $\overline{A * B}$ the filled join of A and B. $K^\diamond$ is defined to be the filled join of the two sets K^+ and K^-. A lower bound for $K^\diamond$ together with the subset relation $K^\diamond \subset K \times K^\circ$ reveals a lower bound for the Mahler volume.

3.3 Families for which the Mahler's conjecture is proved

There are two families of bodies for which the conjecture has been proved succesfully. Saint-Raymond [22] proves the conjecture for unit balls of Banach spaces with a 1-unconditional basis and Reisner [18] for Zonoids.

That the convex body is a unit ball of a Banach space is not a strict restriction. Having any convex body in $\mathbb{R}^n$ we can realize the corresponding Banach space as $\mathbb{R}^n$ equipped with the gauge function of the body as norm. The body we started with is now the unit ball in the new Banach space. That the Banach space has a 1-unconditional basis means that there is a basis $\big\{x_i\big\}_{i=1}^n$ such that

$$\left|\left| \sum_{i=1}^{n} \alpha_i x_i \right|\right|_{g(x)} = \left|\left| \sum_{i=1}^{n} \epsilon_i \alpha_i x_i \right|\right|_{g(x)} \tag{42}$$

holds for all scalars $\{\alpha_i\}_{i=1}^n$ and all signs $\{\epsilon_i\}_{i=1}^n$, $\epsilon_i = \pm 1$ [20]. In geometric terms this says that the body has to be symmetric to all coordinate hyperplanes [26].

Zonoids are limits of zonotopes in the Hausdorff topology and zonotopes themselves are Minkowski sums of intervals. The first proof that Reisner gives [18] as well as the paper were he states the cases in which equality is obtained [19] use probabilistic

arguments involving random hyperplanes. Equality is proved to be obtained if and only if the zonoid is a parallelotope. There is also a simplified version of the proof by Gordon, Meyer and Reisner [8] that uses mainly geometric arguments.

3.4 Necessary conditions on the minimizer of the Mahler volume

Not much is known about the minimizer of the Mahler volume. Stancu [25] shows that the minimizer cannot have a boundary of class C^2 with everywhere positive Gauss curvature. The proof shows that for sufficient small values of modification the floating and illumination body of a convex body of class C^2_+ have smaller, respective bigger, Mahler volume than the original body. Furthermore the inequalities are sharp if the original body is not an ellipsoid.

CHAPTER IV

CALCULATING THE MAHLER VOLUME

To examine Mahler's conjecture about the volume product we need formulas to calculate the volume of a given symmetric convex body $K \in \mathbb{K}^n$ and its dual. We like to represent the body with its support function h_K. We fix that notation and in the whole chapter K will be a convex body and h its support function. Additionally we want to be able to modify a given support function with small pertubations to determine if the starting body is a local minimum of the Mahler volume. For these purposes the formulas have to be numerically efficient to calculate.

Note that choosing the gauge function g_K as representation of the body would yield the same results since this function is the support function of the dual body K° and by Proposition 2.1.2 $M(K) = M(K^\circ)$. Having the support function on hand it is easier to calculate the volume of the dual body. So this chapter is organized as follows: We first introduce some further notation followed by formulas to calculate the volume of the dual body. We then give formulas for the volume of the original body. We will derive the formulas for $\mathbb{R}^n$ whenever possible but our numerical calculations will focus on the first open case $n = 3$. So the formulas will be specialized for that case to make it easier to reproduce the numeric calculations.

4.1 Usage of spherical corrdinates

We will use spherical coordinates and for $\mathbb{R}^3$ these coordinates are set to correspond to the radial distance r, the colatitude θ from 0 to π and the longitude φ ranging from 0 to 2π. For $\mathbb{R}^3$ we hence have the standard cartesian coordinates x, y, z expressed in spherical coordinates as $x = r\cos(\varphi)\sin(\theta),\ y = r\sin(\varphi)\sin(\theta),\ z = r\cos(\theta)$.

As the support and the gauge function can be viewed as functions on the unit sphere

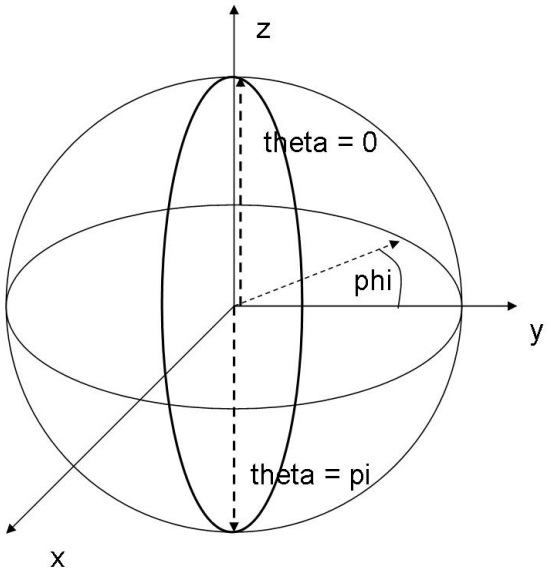

Figure 8: The spherical coordinate system in $\mathbb{R}^3$

we will often refer to them as functions of a unit vector ω and in the case of 3 dimensions as functions of the angles θ and φ and write $h(\omega)$ and $h(\theta, \varphi)$ respectively. Sometimes we want to use spherical coordinates but need the functions to be defined on the whole space. With the positive homogeneity of degree 1 the functions are easily extended and will be written as $h(r, \omega) = r\, h(\omega)$ and $h(r\theta, \varphi) = r\, h(\theta, \varphi)$ for $\mathbb{R}^n$ and $\mathbb{R}^3$ respectively.

We will use the transformation from cartesian to spherical coordinates which has as inverse of the determinant of the Jacobian matrix r^{n-1} when performed in $\mathbb{R}^n$. The standard Lebesgue measure will be denoted dV and the spherical Lebesgue measure $d\omega$ in arbitrary dimensions. So the transformation between these two measure can be written as

$$dV = r^{n-1}\, d\omega \tag{43}$$

with

$$d\omega = \sin(\theta) d\theta d\varphi \tag{44}$$

in $\mathbb{R}^3$. The unit sphere in $\mathbb{R}^n$ is denoted by S^{n-1}.

4.2 Calculating the volume of the dual body

4.2.1 The basic formula for the volume of the dual body

Theorem 4.2.1 (The basic formula for the volume of the dual body):

Given a convex body K and its support function h the volume of its dual body is given by

$$V(K^\circ) = \frac{1}{n}\int_{\omega\in S^{n-1}} h(\omega)^{-n} d\omega;. \tag{45}$$

This equation becomes

$$V(K^\circ) = \frac{1}{3}\int_0^{2\pi}\int_0^{\pi} h^{-3}(\theta,\varphi)\sin(\theta)\, d\theta\, dphi \tag{46}$$

in $\mathbb{R}^3$.

Proof. The support function of the body is the gauge function of the dual body. So we can look at K° as $K^\circ = \{x \in \mathbb{R}^n : \ h(x) \leq 1\}$ and its boundary is defined by $\partial K^\circ = \{x \in \mathbb{R}^n : \ h(x) = 1\}$. So for any $\omega \in S^{n-1}$ we get that $\frac{\omega}{h(\omega)} \in \partial K^\circ$, since $h\big(\frac{\omega}{h(\omega)}\big) = \frac{h(\omega)}{h(\omega)} = 1$. This justifies the boundaries of integration for transformation from cartesian to spherical coordinates:

$$\begin{aligned} V_n(K^\circ) = \int_{K^\circ} dV &= \int_{\omega\in S^{n-1}}\int_0^{\frac{1}{h(\omega)}} r^{n-1} dr\, d\omega = \\ &= \int_{\omega\in S^{n-1}} \left[\frac{r^n}{n}\right]_{r=0}^{r=\frac{1}{h(\omega)}} d\omega = \frac{1}{n}\int_{\omega\in S^{n-1}} h(\omega)^{-n} d\omega\ . \end{aligned}$$

Specializing this equation to $\mathbb{R}^3$ we get

$$V_3(K^\circ) = \frac{1}{3}\int_{\omega\in S^2} h(\omega)^{-3} d\omega = \int_0^{2\pi}\int_0^{\pi} h^{-3}(\theta,\varphi)\sin(\theta) d\theta\, d\varphi\ .$$

□

4.2.2 A family of formulas for the volume of the dual body

Equation (45) can as well be used to derive a family of formulas for the volume of the dual body. Therefore we will use the following coordinate transformation T

from spherical coordinates (r, ω) to coordinates given by $\big(h(r,\omega), \omega\big)$ for $\omega \in S^{n-1}$. To calculate the Jacobian J_T of this transformation we introduce another function $R(\omega) := \frac{1}{h(1,\omega)}$. With that notation we can use the positive homogeneity of degree 1 of h to rewrite

$$h(r,\omega) = \frac{r}{R(\omega)} \ . \tag{47}$$

Now the Jacobian J_T is given by

$$J_T = \begin{pmatrix} \frac{\partial h(r,\omega)}{\partial r} & \frac{\partial h(r,\omega)}{\partial \omega} \\ \frac{\partial \omega}{\partial r} & \frac{\partial \omega}{\partial \omega} \end{pmatrix} = \begin{pmatrix} \frac{1}{R(\omega)} & -\frac{r}{R^2(\omega)} \frac{\partial R(\omega)}{\partial \omega} \\ 0 & 1 \end{pmatrix} \ ,$$

and the inverse of the determinant of the Jacobian is

$$\det(J)^{-1} = R(\omega) \ . \tag{48}$$

With this transformation and using equations (47) and (43) the standard Lebesgue measure dV becomes

$$dV = r^{n-1} dr \, d\omega = \big(h(r,\omega) R(\omega)\big)^{n-1} R(\omega) dh \, d\omega = h^{n-1}(r,\omega) R^n(\omega) dh \, d\omega \ . \tag{49}$$

This discussion prepares the following theorem.

Theorem 4.2.2 (A family of formulas for the volume of the dual body):

Given a convex body K and its support function h, assume F is a function such that the integral $\int_{\mathbb{R}^n} F(h) dV$ exists. Then the following equation holds

$$V(K^\circ) = \frac{1}{n} \frac{\int_{\mathbb{R}^n} F(h) dV}{\int_0^\infty F(h) h^{n-1} dh} \ , \tag{50}$$

and in particular for $F(\cdot) = e^{\frac{1}{2}(\cdot)^2}$ we get

$$V(K^\circ) = \frac{1}{n} \frac{1}{2^{n/2-1}} \frac{1}{\Gamma\big(\frac{n}{2}\big)} \int_{\mathbb{R}^n} e^{-\frac{1}{2}h^2} dV \ . \tag{51}$$

This equation becomes

$$V(K^\circ) = \frac{1}{3}\sqrt{\frac{2}{\pi}} \int_{-\infty}^{\infty} \int_{-\infty}^{\infty} \int_{-\infty}^{\infty} e^{-\frac{1}{2}h^2(x,y,z)} dx \, dy \, dz \tag{52}$$

when performed in $\mathbb{R}^3$ with cartesian coordinates and

$$V(K^\circ) = \frac{1}{3}\sqrt{\frac{2}{\pi}} \int_0^\infty \int_0^{2\pi} \int_0^\pi e^{-\frac{1}{2}r^2h^2(\theta,\varphi)} r^2 \sin(\theta)\, d\theta\, d\varphi\, dr \tag{53}$$

with spherical coordinates.

Proof. Knowing that the first integral exists we use the transform in (49) to get

$$\begin{aligned}\int_{\mathbb{R}^n} F(h)dV &= \int_{S^{n-1}} \int_0^\infty F(h)h^{n-1}R(\omega)dh\, d\omega = \\ &= \frac{1}{n}\int_{S^{n-1}} R^n(\omega)d\omega \cdot n \int_0^\infty F(h)h^{n-1}dh\ .\end{aligned}$$

By equations (47) and (45) the first integral equals $V(K^\circ)$ and so equation (50) follows. For equation (51) use the variable transformation $\frac{1}{2}h^2 = t \Rightarrow h = \sqrt{2t} \Rightarrow \frac{dh}{dt} = \frac{1}{\sqrt{2t}}$, to calculate

$$\int_0^\infty e^{\frac{1}{2}h^2}h^{n-1}dh = \int_0^\infty e^{-t}\big(\sqrt{2t}\big)^{n-1}\frac{1}{\sqrt{2t}}dt = 2^{n/2-1}\int_0^\infty e^{-t}t^{n/2-1} = 2^{n/2-1}\cdot\Gamma\big(\frac{n}{2}\big)\ .$$

The equations for $\mathbb{R}^3$ simply follow by using $\Gamma\left(\frac{3}{2}\right) = \frac{\sqrt{\pi}}{2}$ and the definitions for the lebesgue measure in the corresponding coordinates. □

4.3 Calculating the volume of the original body

To calculate the volume of the original body there are mainly two distinct approaches. We could either use formulas that directly involve the support function or use Theorem 2.5.3 and the generalized Legendre transform to map the support function of the body to its gauge function. We are then able to use the formulas introduced in Theorem 4.2.1 as the gauge function is the support function of the dual body.

4.3.1 Using the Legendre transform to calculate the volume of the original body

Let us first look at the generalized Legendre transform and how it can be used to calculate the volume of the the body K. Combining Theorem 2.5.3 with equation 45

yields

$$V_n(K) = \frac{1}{n}\int_{\omega\in S^{n-1}} \left(\sqrt{2\mathcal{L}\Big[\frac{h^2}{2}\Big](\omega)}\right)^{-n} d\omega = \\ = \frac{1}{n}\int_{\omega\in S^{n-1}} \left(2\max_{x\in\mathbb{R}^n}\left\{\langle\omega,x\rangle - \frac{1}{2}h^2(x)\right\}\right)^{-n/2} d\omega\ . \tag{54}$$

Note that the generalized Legendre transform needs to maximize over all of $\mathbb{R}^n$ and not just over the unit sphere S^{n-1}. Looking at that formula one weakness of the approach using the generalized Legendre transform is obvious. The integral is indirectly defined and one either needs to find a closed form for the maximum involved in the calculation or the maximum always has to be evaluated numerically. This calculation will be time consuming. Nevertheless in $\mathbb{R}^3$ we can simplify equation (54) using spherical coordinates and the positive homogeneity of the support function. We use the notation $u(\theta,\varphi) = \begin{pmatrix}\cos(\varphi)\sin(\theta)\\ \sin(\varphi)\sin(\theta)\\ \cos(\theta)\end{pmatrix}$ as abbreviation of the unit vector corresponding to the angles θ and φ. With this shortcut we get

$$V_3(K) = \frac{1}{3}\int_{\omega\in S^2} \left(2\max_{0\le r,\ 0\le\theta\le\pi,\ 0\le\varphi\le 2\pi}\left\{\big\langle\omega, ru(\theta,\varphi)\big\rangle - \frac{1}{2}r^2h^2(\theta,\varphi)\right\}\right)^{-3/2} d\omega = \\ = \frac{1}{3}\int_{\omega\in S^2} \left(2\max_{0\le r,\ 0\le\theta\le\pi,\ 0\le\varphi\le 2\pi}\left\{r\big\langle\omega, u(\theta,\varphi)\big\rangle - \frac{1}{2}r^2h^2(\theta,\varphi)\right\}\right)^{-3/2} d\omega\ . \tag{55}$$

Hereby the function $r\big\langle\omega,u(\theta,\varphi)\big\rangle - \frac{1}{2}r^2h^2(\theta,\varphi)$ over which the maximization is done is a quadratic function in r and for any fixed pair of (θ,φ) and any fixed $\omega\in S^{n-1}$ it is easily checked that it takes its maximum for $r = \frac{\langle\omega,u(\theta,\varphi)\rangle}{h^2(\theta,\varphi)}$. So we substitute that

expression to get

$$V_3(K) = \frac{1}{3}\int_{\omega\in S^2}\left(2\max_{0\le\theta\le\pi,\,0\le\varphi\le 2\pi}\left\{\frac{\langle\omega,u(\theta,\varphi)\rangle}{h^2(\theta,\varphi)}\big\langle\omega,u(\theta,\varphi)\big\rangle - \right.\right.$$
$$\left.\left. - \frac{1}{2}\left(\frac{\langle\omega,u(\theta,\varphi)\rangle}{h^2(\theta,\varphi)}\right)^2 h^2(\theta,\varphi)\right\}\right)^{-3/2} d\omega =$$
$$= \frac{1}{3}\int_{\omega\in S^2}\left(2\max_{0\le\theta\le\pi,\,0\le\varphi\le 2\pi}\left\{\frac{1}{2}\frac{\langle\omega,u(\theta,\varphi)\rangle^2}{h^2(\theta,\varphi)}\right\}\right)^{-3/2} d\omega =$$
$$= \frac{1}{3}\int_{\omega\in S^2}\left(\max_{0\le\theta\le\pi,\,0\le\varphi\le 2\pi}\left\{\frac{\langle\omega,u(\theta,\varphi)\rangle}{h(\theta,\varphi)}\right\}\right)^{-3} d\omega\ . \tag{56}$$

This expression is still implicit but it reduces the domain over which the maximization is done by 1 dimension.

Formulas to directly calculate the volume of a body given its support function are more involved than those for the dual body. To introduce them we need more theory from differential geometry which will now be introduced briefly.

4.3.2 Some background in differential geometry and the divergence theorem

To derive direct formulas for the volume of a convex body given its support function we need to know about the divergence theorem, the principal radii of curvature, an equation by Weingarten and the Gauss map. The divergence theorem, often called Gauss's theorem, is a standard result from vector calculus and can e.g. be found in [17] and for the latter three, we refer to [24] for a more rigorous discussion.

The Gauss map G maps a surface M in $\mathbb{R}^n$ continuously to the unit sphere S^{n-1}. A point p on the surface is mapped to its unit normal vector. The Gauss map can be defined globally if and only if the surface is smooth and orientable. For a convex body the Gauss map is defined on ∂K if the body is smooth. The tangent space at the point p is parallel to the tangent space at the image point on the sphere and so the differential dG can be considered as a map of the tangent space at p into itself. The Jacobian of the Gauss map, also called shape operator or Weingarten map, has as its determinant the Gaussian curvature which is the product of the principal curvatures.

The trace of the shape operator is the sum of the principal curvatures. The idea of the principal of curvatures will now be introduced.

Definition 4.3.1 (Curvature of a curve in $\mathbb{R}^2$):

The (extrinsic) curvature κ of a curve γ in $\mathbb{R}^2$ is given by

$$\kappa = \frac{d\theta}{ds} \,, \tag{57}$$

where s is the arc length of the curve and θ the tangential angle.

So the curvature measures how much a curve bends at a certain point. The change

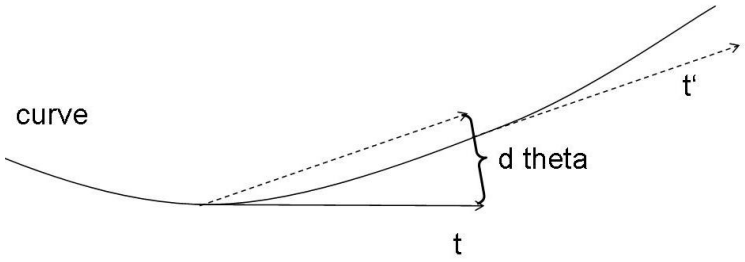

Figure 9: Cuvature measures the change of the tangential angle with respect to arc length

in the angle of the tangential vector t is measured with respect to the change in the arc length of the curve.

The inverse of the curvature is called the radius of curvature

$$R := \frac{1}{\kappa} \ = \frac{ds}{d\theta} \,. \tag{58}$$

The radius of curvature can be seen as the radius of the osculating circle to the curve at a given point p. The osculating circle is the tangential circle on the inside of the curve which approximates the curve "most tightly" at the given point. The curvature of the osculating circle, i.e. the inverse of its radius, is the curvature of the curve at that point.

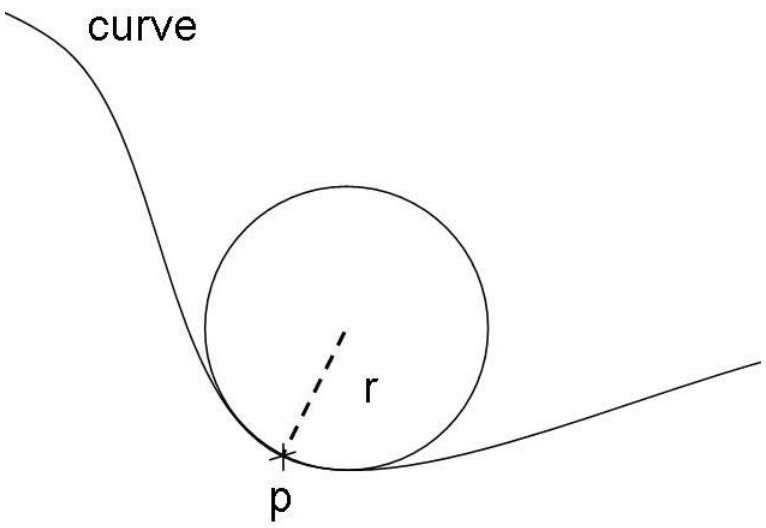

Figure 10: The osculating circle of a curve

To define curvature and the principal radii of curvature in higher dimensions we use the definition of curvature of a curve in $\mathbb{R}^2$. Having a smooth surface M in $\mathbb{R}^3$ and a given point p on that surface there is a unique outward unit normal vector at that point. This vector gives rise to a family of normal planes, which are all planes that contain this unit normal vector. Each of the normal planes contains a unique tangent vector and therefore the normal plan intersects the surface in a plane curve. This curve has a curvature as defined in Definition 4.3.1.

In general this curvature is different for different normal planes intersecting the surface. The principal curvatures of the surface are the maximum and minimum curvatures corresponding to the different normal planes. The principal directions are the normal vectors of the corresponding normal planes.

It is known that the principal directions are the eigenvectors and the principal curvatures are the eigenvalues of the shape operator, also called Weingarten map, which is the differential of the Gauss map. Therefore we know that the planes for which the curvature is maximized and minimized are orthogonal to each other and always exist.

This approach can as well be used to define principal curvatures and directions. In higher dimensions we define the principal curvatures and principal directions to be the eigenvalues and eigenvectors of the shape operator, respectively.

For the Hessian in spherical coordinates the change of variables yields the following formula:

$$\mathcal{H} = \begin{pmatrix} \frac{\partial^2}{\partial\theta^2} & \frac{\partial}{\partial\theta}\frac{1}{\sin(\theta)}\frac{\partial}{\partial\varphi} \\ \frac{\partial}{\partial\theta}\frac{1}{\sin(\theta)}\frac{\partial}{\partial\varphi} & \frac{\cos(\theta)}{\sin(\theta)}\frac{\partial}{\partial\theta} + \frac{1}{\sin^2(\theta)}\frac{\partial^2}{\partial\varphi^2} \end{pmatrix} . \tag{59}$$

This spherical Hessian is closely related to the shape operator. We get that $(\mathcal{H}+1)(h)$ is equivalent to the inverse of the shape operator and hence it has the principal radii of curvature as eigenvalues. So we get for the product of the principal radii of curvature

$$R_1 \cdot R_2 = \det\big((\mathcal{H} + \mathbf{1})h\big) , \tag{60}$$

where $\mathbf{1}$ denotes the identity matrix. Furthermore we can derive the Laplacian Δ in spherical coordinates, which is the trace of $\mathcal{H}(h)$,

$$(\Delta + 2)h = tr\big((\mathcal{H} + \mathbf{1})h\big) = R_1 + R_2 . \tag{61}$$

The explicit form for the Laplacian in spherical coordinates is

$$\Delta = \frac{\partial^2}{\partial\theta^2} + \frac{\cos(\theta)}{\sin(\theta)}\frac{\partial}{\partial\theta} + \frac{1}{\sin^2(\theta)}\frac{\partial^2}{\partial\varphi^2} . \tag{62}$$

We know go back to $\mathbb{R}^2$ to relate the support function and its derivatives to the radius of curvature.

Theorem 4.3.2 (An equation by Weingarten):

For a smooth convex body $K \subset \mathbb{R}^2$ and its support function $h(\theta)$ the following equation holds

$$h(\theta) + h''(\theta) = R(\theta) , \tag{63}$$

with $R(\theta)$ as the curvature at the point, where the support line with normal angle θ touches the body.

Proof. At any angle θ we have $h(\theta) = \langle x_{contact}, \hat{n}(\theta)\rangle$ with $\hat{n}(\theta) = \begin{pmatrix}\cos(\theta)\\ \sin(\theta)\end{pmatrix}$ the normal with respect to θ in cartesian coordinates and $x_{contact}$ the point where the support line of normal $\hat{n}(\theta)$ touches the body. Therefore we get

$$h'(\theta) = \frac{h(\theta)}{d\theta} = \frac{\langle x, \hat{n}\rangle}{d\theta} = \left\langle \frac{dx}{d\theta}, \hat{n} \right\rangle + \left\langle x, \frac{d\hat{n}}{d\theta} \right\rangle =$$
$$= \left\langle \frac{dx}{ds}\frac{ds}{d\theta}, \hat{n} \right\rangle + \langle x, \hat{t}\rangle = \left\langle \hat{t}\,\frac{ds}{d\theta}, \hat{n} \right\rangle + \langle x, \hat{t}\rangle = \langle x, \hat{t}\rangle \ ,$$

with $\hat{t}(\theta) = \begin{pmatrix}-\sin(\theta)\\ \cos(\theta)\end{pmatrix} = \frac{d\hat{n}}{d\theta}$ the unit tangent vector corresponding to $x_{contact}$. Another differentiation yields

$$h''(\theta) = \frac{\langle x, \hat{t}\rangle}{d\theta} = \left\langle \frac{dx}{d\theta}, \hat{t} \right\rangle + \left\langle x, \frac{d\hat{t}}{d\theta} \right\rangle = \left\langle \frac{dx}{ds}\frac{ds}{d\theta}, \hat{t} \right\rangle + \langle x, -\hat{n}\rangle =$$
$$= \langle \hat{t}R, \hat{t}\rangle - \langle x, \hat{n}\rangle = R\,||\hat{t}||^2 - h(\theta) = R - h(\theta)$$

□

The last fact we pull from differential geometry is the divergence theorem.

Theorem 4.3.3 (Divergence Theorem):

For any subset $V \subset \mathbb{R}^n$ that is compact and has a piecewise smooth boundary and any vector field F which is continuously differentiable on a neighborhood of V, the equation

$$\int_V \langle \nabla, F\rangle dV = \int_{\partial V} \langle F, \hat{n}\rangle da \tag{64}$$

holds. da hereby stands for the surface area measure and $\hat{n}$ for the unit outward normal corresponding to the point on the surface over which we integrate.

Note further that the divergence of the identity vector field in n dimensions equals n, i.e.

$$\langle \nabla, x\rangle = n \ . \tag{65}$$

We are now ready to introduce direct formulas for the volume of the original body.

4.3.3 Direct formulas for the volume of the original body

Theorem 4.3.4 (A direct formula for the volume of the original body): Given a smooth convex body $K \in \mathbb{K}^n$ by its support function h its volume is given by

$$V(K) = \frac{1}{n} \int_{S^{n-1}} h(\omega) \prod_{i=1}^{n-1} R_i(\omega)\, d\omega \,, \tag{66}$$

where R_i denote the $n-1$ principal radii of curvature.

With the spherical Hessian this formula becomes

$$V(K) = \frac{1}{3} \int_0^{2\pi} \int_0^{\pi} h(\theta,\varphi) \det\left[\mathcal{H}(h(\theta,\varphi)) + \mathbf{1}(h(\theta,\varphi))\right] \sin(\theta)\, d\theta\, d\varphi \tag{67}$$

in $\mathbb{R}^3$.

Proof. While n denotes the dimension, $\hat{n}$ is the outward unit normal corresponding to the point x on the surface of K. With that we get

$$\begin{aligned} V(K) &= \frac{1}{n} \int_K \langle \nabla, x \rangle \, dV = \frac{1}{n} \int_{\partial K} \langle x, \hat{n} \rangle \, da = \frac{1}{n} \int_{\partial K} \hat{h}(x)\, da = \\ &= \frac{1}{n} \int_{S^{n-1}} h(\omega) \prod_{i=1}^{n-1} R_i(\omega)\, d\omega \,, \end{aligned}$$

where the first equal sign is due to equation (65) and for the second one we apply the divergence theorem. $\hat{h}(x)$ introduces another parametrization of the support function. $\hat{h}(x)$ is the support function evaluated at the angle $\omega_x = \hat{n_x}$ which corresponds to the outward unit normal at the point x. Hence he have $\hat{h}(x) = h(\omega_x) = \langle x, \hat{n} \rangle$. The last equal sign uses the transformation given by the Gauss map to change the area of integration from ∂K to the unit sphere. The determinant of the inverse of the Gauss map equals the product of the principal radii of curvature. The formula using the spherical Hessian now follows from equation (60). □

CHAPTER V

EXPERIMENTAL RESULTS

In this chapter we discuss the experiments performed and the results we got. All experiments are done in $\mathbb{R}^3$ and so the discussion focuses on that case. First the different formulas to calculate the volume of the body and its dual introduced in Sections 4.3 and 4.2 are evaluated for the cube, the cross polytope and the ball. Their performance will be compared and advantages and disadvantages of the different formulas will be discussed. Before continuing with the actual experiments we introduce formulas to visualize the body and its dual given the support function. Then the spherical harmonics, which form a basis for the set of square integrable functions over S^2, are presented. This discussion prepares the further experiments. The cube and the cross polytope are approximated by their spherical harmonic expansion and the performance of this approximation is rated. We finish this section with another approximation of the cube. Its radii of curvature functions, which are Dirac-δ functions, are approximated and so a body similar to the cube is generated.

The calculations in that chapter are performed in Mathematica [30] and the notebook including the calculations is attached in the appendix. By evaluating the notebook all results and graphics are be generated and are available for in depth analysis.

5.1 Performance tests of the formulas for the Mahler volume

In this section we test the different formulas introduced in Chapter 4 to calculate the volume of a body and its dual given the support function of the body. We begin by testing the formulas for the dual body and then discuss the formulas for the original body.

5.1.1 Testing the formulas for the volume of the dual body

We begin with testing the formulas for the volume of the dual body introduced in Section 4.2. These formulas are:

- (46): Basic Spher. Coord.: $\frac{1}{3}\int_0^{2\pi}\int_0^{\pi} h^{-3}(\theta,\varphi)\sin(\theta)\,d\theta\,d\varphi$
- (53): Exp. Spher. Coord.: $\frac{1}{3}\sqrt{\frac{2}{\pi}}\int_0^{\infty}\int_0^{2\pi}\int_0^{\pi} e^{-\frac{1}{2}r^2h^2(\theta,\varphi)}r^2\sin(\theta)\,d\theta\,d\varphi\,dr$
- (52): Exp. Cart. Coord.: $\frac{1}{6}\sqrt{\frac{2}{\pi}}\int_{-\infty}^{\infty}\int_{-\infty}^{\infty}\int_{-\infty}^{\infty} e^{-\frac{1}{2}h^2(x,y,z)}dx\,dy\,dz$

To benchmark the different formulas we will evaluate them on calculating the volumes of the conjectured extreme cases of the Mahler volume, the cube, the cross polytope and the sphere. Additionally we perform two different kinds of calculations: First we ask Mathematica to calculate the corresponding integral symbolically. Secondly the integral should be evaluated numerically. The results obtained as well as the running times for both calculations are summarized in Tables 2 and 3, respectively. In the columns the calculated volumes of the dual bodies are grouped with the running time for that body and algorithm. Hereby I^3 stands for the cube, O^3 for the cross polytope, in three dimensions called octahedron, and B^3 for the ball. Note that the we calculate the volume of the dual body, and so we get $V((I^3)^\circ) = \frac{4}{3}$ and not 8. The calculations were performed on a 2 GHz proecssor.

Table 2: Comparing the exact results of the different formulas for the volume of the dual body

Formula	$V((I^3)^\circ)$	time [s]	$V((O^3)^\circ)$	time [s]	$V((B^3)^\circ)$	time [s]
exact value	$\frac{4}{3}$	n.a.	8	n.a.	$\frac{4}{3}\pi$	n.a.
basic spher. cord.	$\frac{4}{3}$	25.1	8	592	$\frac{4}{3}\pi$	0.047
exp. spher. cord.	*n.a.*	*n.a.*	*n.a.*	*n.a.*	$\frac{4}{3}\pi$	0.20
exp. cart. cord.	$\frac{4}{3}$	16.3	8	14.4	$\frac{4}{3}\pi$	0.52

Table 3: Comparing the numeric results of the different formulas for the volume of the dual body

Formula	$V((I^3)^\circ)$	time [s]	$V((O^3)^\circ)$	time [s]	$V((B^3)^\circ)$	time [s]
exact value	$\frac{4}{3}$	n.a.	8	n.a.	≈ 4.188790	n.a.
basic spher. cord.	1.33333	1.139	8	5.039	4.18879	10^{-17}
exp. spher. cord.	1.33333	5.584	8	7.753	4.18879	0.031
exp. cart. cord.	1.33333	0.218	8	0.344	4.18879	0.546

Looking at the results we first notice that all calculated results are correct. Nevertheless not all calculations terminated. The exponential formula using spherical coordinates was neither able to calculate the exact volume of the ball nor of the cross polytope. Staying with the exact calculations we see that the exponential formula in cartesian coordinates beats the basic formula in spherical coordinates in terms of running time. For the cube the basic formula needs 1.7 and for the cross polytope even over 40 times the running time of the exponential formula with cartesian coordinates. For the ball the basic formula is faster by a factor 10, which is evidently because the integals are just evaluated over a constant function.

Looking at the numerical calculations the results are similar. The exponential formula with cartesian coordinates beats the basic formula in spherical coordinates by a factor of 5 and 15 in running time for the cube and cross polytope, respectively. For the ball the basic formula using spherical coordinates is again superior since it just has to evaluate a constant integral. The exponential formula using spherical coordinates is able to produce numeric results, but it is slower than the basic formula in the same coordinate system.

In conclusion we see that the exponential formula in cartesian coordinates is in general faster than the basic formula in spherical coordinates. So if we have the choice between the support function in cartesian and spherical coordinates we should stick with the cartesian coordinate system and use the exponential formula. If we do not

have the choice of the coordinate system and have to stick with spherical coordinates, we should take advantage of the basic formula.

5.1.2 Testing the formulas for the volume of the original body

The formulas for the volume of the original body have been introduced in Section 4.3 and are:

- (54): Leg. Cart. Coord.: $\frac{1}{3}\int_{\omega\in S^2}\left(2\max_{x\in\mathbb{R}^n}\left\{\langle\omega,x\rangle-\frac{1}{2}h^2(x)\right\}\right)^{-3/2}d\omega$
- (55): Leg. Spher. Coord.: $\frac{1}{3}\int_{\omega\in S^2}\Big(2\max_{0\le r,\,0\le\theta\le\pi,\,0\le\varphi\le2\pi}\left\{r\langle\omega,u(\theta,\varphi)\rangle-\right.$
$\left.-\frac{1}{2}r^2h^2(\theta,\varphi)\right\}\Big)^{-3/2}d\omega$
- (56): Simply. Leg. Spher. Coord.: $\frac{1}{3}\int_{\omega\in S^2}\left(\max_{0\le\theta\le\pi,\,0\le\varphi\le2\pi}\left\{\frac{\langle\omega,u(\theta,\varphi)\rangle}{h(\theta,\varphi)}\right\}\right)^{-3}d\omega$
- (67): Spher. Hess.: $\frac{1}{3}\int_{S^2}h(\omega)\det\left[\mathcal{H}(h(\omega))+\mathbf{1}(h(\omega))\right]d\omega$

The formula using the spherical Hessian requires the body to be smooth. One the one hand this is required by the techniques used to deduce it, by the divergence theorem and the Gauss map. On the other side the radii of curvature are infinity for a flat side of the body and 0 for corners. For the cube and the cross polytope the corners correspond to almost every angle of the support plane normals. So the integrals involved evaluate to 0. Consequently the formula using the Spherical Hessian is not suitable to calculate the volume of the cube or the cross polytope.

The three formulas using the Legendre transform encounter another problem. In no version of this formula we are able to find a closed expression for the maximum involved in these formulas and so all integrals have to be evaluated numerically. But this means that for each sampling point of the numeric integration this maximum has to be evaluated numerically. To be exact the numeric integration needs many sample points and so this maximum has to be calculated very often. The formula using the Legendre transformation in Cartesian coordinates is able to calculate the volume of the ball in 19 seconds but it takes 3 days and 3.5 hours to calculate the

volume of the cube with a 3 digit accuracy. The calculations for the cross polytope did not finish. The Legendre transform of the ball is again the identity, so that this calculation finishes fast. Taking more than 3 days to calculate the volume of the cube, this formulas is not useful for testing a lot of random guesses for potential minimizers. The formulas using the Legendre transform in spherical coordinates were not able to calculate any of the requested volumes correctly. Presumably they are having problems to evaluate the maximum for the sample points of the numeric integration. In short the formulas using the Legendre transform are not efficient enough for numeric integration and the formula with the spherical Hessian requires a smooth body. So for all smooth bodies we have a way to calculate the volume of the original body. This formula also proves efficient, as we will see when we calculate the Mahler volume of the cube and cross polytope approximated by their spherical harmonic expansion. Nevertheless the formula using the Legendre transform in Cartesian coordinates can still be used to calculate the Mahler volume. Although it is not suitable to test a lot of bodies, it can be used if we have a good guess about which body should have a smaller Mahler volume than the cube. Before we start with approximating the cube and the cross polytope with their spherical harmonic expansion we first introduce some useful formulas and further background.

5.2 Formulas to visualize K and K°

Having the support function of a body it would be nice to know how the body looks. The support function $h(\theta, \varphi)$ describes the distance of the support line of normal $u(\theta, \varphi) = \begin{pmatrix} \cos(\varphi)\sin(\theta) \\ \sin(\varphi)\sin(\theta) \\ \cos(\theta) \end{pmatrix}$ to the origin. The angles θ and φ must not be mixed with the polar angles of the point $x_{contact}$ where the plane supports the body. Although the support function does not directly describe the position of this point, we can relate it to the contact point.

Theorem 5.2.1 (Coordinates of the contact point corresponding to the plane with normal $u(\theta,\varphi)$):

For any smooth $K \in \mathbb{K}^3$ and its support function h the point $x_{contact}(\theta,\varphi)$ where the support plane with normal $u(\theta,\varphi)$ touches the body is given by

$$x_{contact}(\theta,\varphi) = \begin{pmatrix} h(\theta,\varphi)\cos(\varphi)\sin(\theta) + \frac{\partial h(\theta,\varphi)}{\partial\theta}\cos(\varphi)\cos(\theta) - \frac{\partial h(\theta,\varphi)}{\partial\varphi}\frac{\sin(\varphi)}{\sin(\theta)} \\ h(\theta,\varphi)\sin(\varphi)\sin(\theta) + \frac{\partial h(\theta,\varphi)}{\partial\theta}\sin(\varphi)\cos(\theta) - \frac{\partial h(\theta,\varphi)}{\partial\varphi}\frac{\cos(\varphi)}{\sin(\theta)} \\ h(\theta,\varphi)\cos(\theta) - \frac{\partial h(\theta,\varphi)}{\partial\theta}\sin(\theta) \end{pmatrix}. \quad (68)$$

Proof. Having the normal $u(\theta,\varphi) = \begin{pmatrix} \cos(\varphi)\sin(\theta) \\ \sin(\varphi)\sin(\theta) \\ \cos(\theta) \end{pmatrix}$ we get an orthonormal basis of $\mathbb{R}^3$ when adding the two vectors

$$t_1(\theta,\varphi) = \begin{pmatrix} \cos(\varphi)\cos(\theta) \\ \sin(\varphi)\cos(\theta) \\ -\sin(\theta) \end{pmatrix}, \qquad t_2 = \begin{pmatrix} -\sin(\varphi) \\ \cos(\varphi) \\ 0 \end{pmatrix}.$$

It is easily checked that $\frac{\partial u(\theta,\varphi)}{\partial\theta} = t_1(\theta,\varphi)$ and $\frac{\partial u(\theta,\varphi)}{\partial\varphi} = \sin(\theta)t_2(\theta,\varphi)$. Additionally the partial differentials $\frac{\partial h(\theta,\varphi)}{\partial(\theta)}$ and $\frac{\partial h(\theta,\varphi)}{\partial\varphi}$ yield vectors in the tangent space of the contact point, which are thus orthogonal to the normal $u(\theta,\varphi)$. In fact these differentials are given by the above introduced tangent vectors t_1 and t_2. As in the proof of the equation by Weingarten in Theorem 4.3.2, we calculate the derivates of $h(\theta,\varphi)$ with respect to θ and φ:

$$\begin{aligned} \frac{\partial h(\theta,\varphi)}{\partial\theta} &= \frac{\partial}{\partial\theta}\big\langle x_{contact}(\theta,\varphi), u(\theta,\varphi)\big\rangle = \\ &= \big\langle \frac{\partial}{\partial\theta}x_{contact}(\theta,\varphi), u(\theta,\varphi)\big\rangle + \big\langle x_{contact}(\theta,\varphi), \frac{\partial}{\partial\theta}u(\theta,\varphi)\big\rangle = \\ &= 0 + \langle x_{contact}(\theta,\varphi), t_1(\theta,\varphi)\rangle = \langle x_{contact}(\theta,\varphi), t_1(\theta,\varphi)\rangle \end{aligned}$$

$$\begin{aligned}\frac{\partial h(\theta,\varphi)}{\partial \varphi} &= \frac{\partial}{\partial \varphi}\big\langle x_{contact}(\theta,\varphi), u(\theta,\varphi)\big\rangle = \\ &= \big\langle \frac{\partial}{\partial \varphi} x_{contact}(\theta,\varphi), u(\theta,\varphi)\big\rangle + \big\langle x_{contact}(\theta,\varphi), \frac{\partial}{\partial \varphi} u(\theta,\varphi)\big\rangle = \\ &= 0 + \langle x_{contact}(\theta,\varphi), \sin(\theta) t_2(\theta,\varphi)\rangle = \langle x_{contact}(\theta,\varphi), \sin(\theta) t_2(\theta,\varphi)\rangle\end{aligned}$$

With u, t_1, t_2 as on orthonormal basis of $\mathbb{R}^3$ we can decompose the point of contact as

$$\begin{aligned}x_{contact} &= \langle x_{contact}, u\rangle u + \langle x_{contact}, t_1\rangle t_1 + \langle x_{contact}, t_2\rangle t_2 = \\ &= h \cdot u + \frac{\partial h}{\theta} \cdot t_1 + \frac{\partial h}{\varphi} \frac{1}{\sin(\theta)} \cdot t_2 \ .\end{aligned}$$

The desired result now follows when plugging in the values of $u(\theta,\varphi)$, $t_1(\theta,\varphi)$ and $t_2(\theta,\varphi)$. □

With the just introduced formula for the point of contact we have a representation of ∂K in spherical coordinates. This can easily be utilized to plot the body. Visualizing the dual body is easier since the angles (θ,φ) used in the gauge function directly describe the angles of the corresponding boundary point.

Theorem 5.2.2:

For any $K \in \mathbb{K}^3$ and its support function h we can represent $\partial(K^\circ)$ in spherical coordinates as

$$k^\circ(\theta,\varphi) = \begin{pmatrix} \frac{1}{h(u(\theta,\varphi))} \cos(\varphi)\sin(\theta) \\ \frac{1}{h(u(\theta,\varphi))} \sin(\varphi)\sin(\theta) \\ \frac{1}{h(u(\theta,\varphi))} \cos(\theta) \end{pmatrix} , \tag{69}$$

where $k^\circ(\theta,\varphi)$ denotes the boundary point of K° in direction $u(\theta,\varphi)$.

Proof. From the positive homogenity of degree 1 of the support function it follows that $h\Big(\frac{u(\theta,\varphi)}{h(u(\theta,\varphi))}\Big) = 1$. Theorem 2.3.5 states that h is the gauge function of K° and hence $\frac{u(\theta,\varphi)}{h(u(\theta,\varphi))} \in \partial K^\circ$. On the other hand it is obvious that $\frac{u(\theta,\varphi)}{h(u(\theta,\varphi))}$ describes the whole boundary of K° since $u(\theta,\varphi)$ covers all of S^2 as θ and φ vary. □

5.3 Spherical harmonics and the expansion of the support and gauge function

Similar to the functions $\left\{e^{inx}\right\}_{n=-\infty}^{n=\infty}$, which are an orthonormal basis for the square integrable functions over S^1 and build the basis for the Fourier series, we now introduce an orthonormal basis for square integrable functions over S^2.

Definition 5.3.1 (Spherical harmonics [1]):

For $n \in \mathbb{N}$ the Legendre polynomials P_n are defined by Rodrigues' Formula as

$$P_n(x) = \frac{1}{2^n n!} \frac{d^n}{dx^n} \left[(x^2 - 1)^n \right] .$$

With that the associated Legendre polynomials P_ℓ^m for $\ell \in \mathbb{N}$ and $m \in \{0, 1, 2, \ldots, \ell\}$ are

$$P_\ell^m(x) = (-1)^m (1 - x^2)^{m/2} \frac{d^m}{dx^m} \big(P_\ell(x) \big) ,$$

and we get negative m by the formula

$$P_\ell^{-m}(x) = (-1)^m \frac{(\ell - m)!}{(\ell + m)!} P_\ell^m(x), \quad m \in \mathbb{N} .$$

Finally we can define the spherical harmonics Y_ℓ^m for $\ell \in \mathbb{N}$ and $m \in \{-\ell, \ldots, \ell\}$ as

$$Y_\ell^m(\theta, \varphi) = \sqrt{\frac{2\ell + 1}{4\pi} \frac{(\ell - m)!}{(\ell + m)!}} \, P_\ell^m(\cos\theta) \, e^{im\varphi} . \tag{70}$$

Theorem 5.3.2 (The spherical harmonics as an orthonormal basis [9]):

The spherical harmnonics Y_ℓ^m are orthonormal, i.e.

$$\int_{S^2} Y_\ell^m Y_{\ell'}^{m'} \, d\omega = \delta_{ll'} \delta_{mm'} \tag{71}$$

where δ_{ij} stands for the Kronecker delta.

Furthermore the spherical harmonics $\left\{ \{Y_\ell^m\}_{m=-\ell}^{m=\ell} \right\}_{\ell=0}^{\ell=\infty}$ are complete in the Hilbert space of square integrable functions over the unit sphere S^2 with the usual inner product $\langle f, g \rangle = \int_{S^2} f \cdot \overline{g} \, d\omega$. Here $\overline{(\cdot)}$ stands for the complex conjugate. Hence Y_ℓ^m

form a basis of that Hilbert space. This means we can write any square integrable function f over S^2 as

$$f(\theta,\varphi) = \sum_{\ell=0}^{\infty} \sum_{m=-\ell}^{\ell} c_\ell^m Y_\ell^m(\theta,\varphi) \tag{72}$$

where

$$c_\ell^m = \int_0^{2\pi} \int_0^{\pi} f(\theta,\varphi)\overline{Y_\ell^m(\theta,\varphi)} \sin(\theta)\, d\theta\, d\varphi \ . \tag{73}$$

The expansion given in equation (72) holds in the sense of that Hilbert space, i.e. in the L^2 sense.

It is known that the spherical harmonics are eigenfunctions of Laplace operator in spherical coordinates and the eigenvalues are given by

$$\Delta Y_\ell^m = -\ell(\ell+1) Y_\ell^m \ . \tag{74}$$

Having the expansion in spherical harmonics of the support function h and of both radii of curvature functions R_1 and R_2 we can use equations (61) and (74) to relate their coefficients. Assuming $h = \sum_{\ell=0}^{\infty} \sum_{m=-\ell}^{\ell} h_\ell^m Y_\ell^m$, $R_1 = \sum_{\ell=0}^{\infty} \sum_{m=-\ell}^{\ell} (r_1)_\ell^m Y_\ell^m$ and $R_2 = \sum_{\ell=0}^{\infty} \sum_{m=-\ell}^{\ell} (r_2)_\ell^m Y_\ell^m$, we get

$$h_\ell^m = \frac{(r_1)_\ell^m + (r_2)_\ell^m}{2 - \ell(\ell+1)} \ , \quad l \neq 1 \ . \tag{75}$$

The functions used for the spherical harmonics expansion oscillate faster and faster as the coefficients increase. A higher ℓ results in a higher order cos term which is equivalent to a linear combination of cos terms with shorter periods. Increasing m results in a faster oscillating $e^{im\varphi}$ term. As we need to combine these functions the spherical harmonic expansion will indeed be a smooth function but one whose behavior is kind of wild even for small neighborhoods. Therefore we expect that the numeric calculations will just be efficient up to a certain amount of coefficients and spherical harmonics used. After that the numeric precision used may not be good enough to capture the wild behavior of the function and the results obtained may no longer make sense.

With this warning in mind, we calculate the coefficients of the spherical harmonic expansion of the cube and the cross polytope support functions and evaluate them for different amounts of coefficients used.

5.4 Approximating the cube and the cross polytope by their spherical harmonic expansions

The cube and cross polytope support functions were introduced in equations (12) and (13) and their spherical harmonic coefficients are calculated up to $\ell = 60$ for all m and the results up to $\ell = 12$ are summarized in Table 4. For the cube the coefficients were calculated exactly but for the cross polytope exact calculations were not successful. The maximum involved in the definition of the cross support function makes a closed integration more difficult. Instead the coefficients were approximated by a numeric integration.

Table 4: The first coefficients of the cube and cross polytope support functions in spherical harmonic expansion

Coefficients of the cube support function calculated exactly

	$m=-12$	$m=-8$	$m=-4$	$m=0$	$m=4$	$m=8$	$m=12$
$l=$				$3\sqrt{\pi}$			
$l=2$				$0\quad 0\quad 0$			
$l=4$			$-\frac{1}{32}\sqrt{\frac{35\pi}{2}}\quad 0\quad 0\quad 0\quad 0$	$-\frac{7\sqrt{\pi}}{32}\quad 0\quad 0\quad 0\quad 0$	$-\frac{1}{32}\sqrt{\frac{35\pi}{2}}$		
$l=6$		$0\quad 0\quad 0$	$-\frac{3}{512}\sqrt{\frac{91\pi}{2}}\quad 0\quad 0\quad 0$	$\frac{3\sqrt{13\pi}}{512}\quad 0\quad 0\quad 0$	$-\frac{3}{512}\sqrt{\frac{91\pi}{2}}\quad 0\quad 0$		
$l=8$		$-\frac{3\sqrt{\frac{12155\pi}{2}}}{8192}\quad 0\quad 0\quad 0$	$-\frac{3\sqrt{\frac{1309\pi}{2}}}{4096}\quad 0\quad 0\quad 0$	$-\frac{99\sqrt{17\pi}}{8192}\quad 0\quad 0\quad 0$	$-\frac{3\sqrt{\frac{1309\pi}{2}}}{4096}\quad 0\quad 0\quad 0$	$-\frac{3\sqrt{\frac{12155\pi}{2}}}{8192}$	
$l=10$		$0\quad 0\quad 0\quad 0$	$-\frac{7\sqrt{\frac{85085\pi}{6}}}{65536}\quad 0\quad 0\quad 0$	$-\frac{7\sqrt{\frac{5005\pi}{2}}}{32768}\quad 0\quad 0\quad 0$	$\frac{455\sqrt{\frac{7\pi}{3}}}{65536}\quad 0\quad 0\quad 0$	$-\frac{7\sqrt{\frac{5005\pi}{2}}}{32768}\quad 0\quad 0\quad 0$	$-\frac{7\sqrt{\frac{85085\pi}{6}}}{65536}\quad 0\quad 0$
$l=12$	$-\frac{15\sqrt{676039\pi}}{1048576}$	$0\quad 0\quad 0\quad -\frac{15\sqrt{\frac{138567\pi}{2}}}{524288}\quad 0\quad 0\quad 0$	$-\frac{225\sqrt{1001\pi}}{1048576}\quad 0\quad 0\quad 0$	$-\frac{11145\sqrt{\pi}}{524288}\quad 0\quad 0\quad 0$	$-\frac{225\sqrt{1001\pi}}{1048576}\quad 0\quad 0\quad 0$	$-\frac{15\sqrt{\frac{138567\pi}{2}}}{524288}\quad 0\quad 0\quad 0$	$-\frac{15\sqrt{676039\pi}}{1048576}$

Coefficients of the cross polytope support function calculated numerically

	$m=-12$	$m=-8$	$m=-4$	$m=0$	$m=4$	$m=8$	$m=12$
$l=0$				2.94649			
$l=2$				$0\quad 0\quad 0$			
$l=4$			0.155025 $\quad 0\quad 0\quad 0$	0.259406 $\quad 0\quad 0\quad 0$	0.155025		
$l=6$		$0\quad 0\quad 0$	0.01394 $\quad 0\quad 0\quad 0$	$-0.00745143\quad 0\quad 0\quad 0$	0.01394 $\quad 0\quad 0$		
$l=8$		$-0.0348128\quad 0\quad 0\quad 0$	$-0.0228487\quad 0\quad 0\quad 0$	$-0.0607595\quad 0\quad 0\quad 0$	$-0.0228487\quad 0\quad 0\quad 0$	-0.0348128	
$l=10$		$0\quad 0\quad 0\quad 0$	$-0.0100825\quad 0\quad 0\quad 0$	$-0.00847097\quad 0\quad 0\quad 0$	$0.00840655\quad 0\quad 0\quad 0$	$-0.00847097\quad 0\quad 0\quad 0$	$-0.0100825\quad 0\quad 0$
$l=12$	0.0145697	$0\quad 0\quad 0\quad 0.00260761\quad 0\quad 0\quad 0$	0.0116409 $\quad 0\quad 0\quad 0$	0.0238043 $\quad 0\quad 0\quad 0$	0.0116409 $\quad 0\quad 0\quad 0$	0.00260761 $\quad 0\quad 0\quad 0$	0.0145697

Looking at that table we note that all coefficients corresponding to odd ℓ's are 0. Spherical harmonics for odd ℓ correspond to odd functions, these are functions that change the sign when the argument is reflected at the origin. The Y_ℓ^m for even ℓ correspond to symmetric functions, that is they stay the same if the argument is reflected at the origin. As both the cube and the cross polytope are symmetric with respect to the origin, this result was expected. Furthermore just for $m = 4n,\ n \in \mathbb{Z}$ we get $c_\ell^m \neq 0$. This result seems to capture more about the symmetric structure of both bodies. Effort was made to find a closed form for the coefficients of the cube but no results were obtained. The implicit definition of the spherical harmonics indicate that these coefficients have a complicated structure.

5.4.1 Approximating the cube by its spherical harmonic expansion

Let us now look at the cube and how we can approximate it by its spherical harmonic expansion. Having its support function we use the coefficients given by equation (73) to get an approximation of the support function via equation (72). We then use equations (68) and (69) to plot the body and its dual defined by the spherical harmonic expansion using all coefficients up to $\ell = 0$, 4, 8, 12, 16, 20, 30, 40, 50, 60. The corresponding plots are presented in Figures 11 and 12.

Let us first look at the pictures for the dual body. For small values of ℓ we can see that the bodies are nonconvex. The flats and edges have some parts that are pressed inwards and are concave. As ℓ goes up these dents become smaller and the body straightens out. Another feature that can be examined is that the corners and edges are smooth for small ℓ and become sharper as ℓ increases. While the appearance of the body changes a lot as ℓ increases from 0 to 20, using more coefficients results in almost no noticeable change of the body.

Examining the plots of the original body we first see the irregularities at the edges. It seems that the flats continue onward from the point of their intersection. These

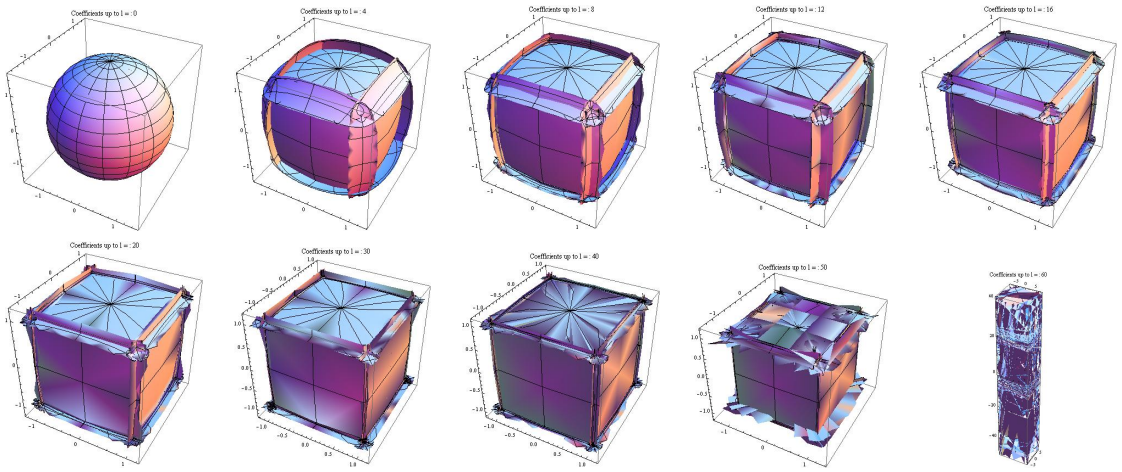

Figure 11: Approximation of the cube by its spherical harmonic expansion for coefficients up to $\ell = 0$, 4, 8, 12, 16, 20, 30, 40, 50, 60

overlaps of the flats become smaller as the number of coefficients increases. Furthermore the first approximating bodies have rounded flats but curvature decreases as ℓ increases. For $\ell = 20$ the flats have almost straightened out and the overlap of the flats has reduced to a small size. Again adding coefficients for $\ell > 20$ does not change the body a lot. When we are using all coefficients up to $\ell = 60$ the result obtained is a numeric artifact. Although we have a lot of zero coefficients in the spherical harmonic expansion as seen in Table 4 we still add up 480 spherical harmonic functions. So presumably the picture generated is a numeric error. Already the picture for $\ell = 50$ shows numeric problems as the overlap of the flats increases and the corners look worse as for smaller ℓ.

To summarize we can say that we have to be careful with approximating the cube with its spherical harmonic expansion. The approximated body itself shows an overlap of the flats and the dual body is nonconvex. But it can as well be seen that these irregularities become smaller as the number of coefficients increases and already for $\ell = 20$ we get results for the approximated cube and its dual that look very similar to the exact bodies.

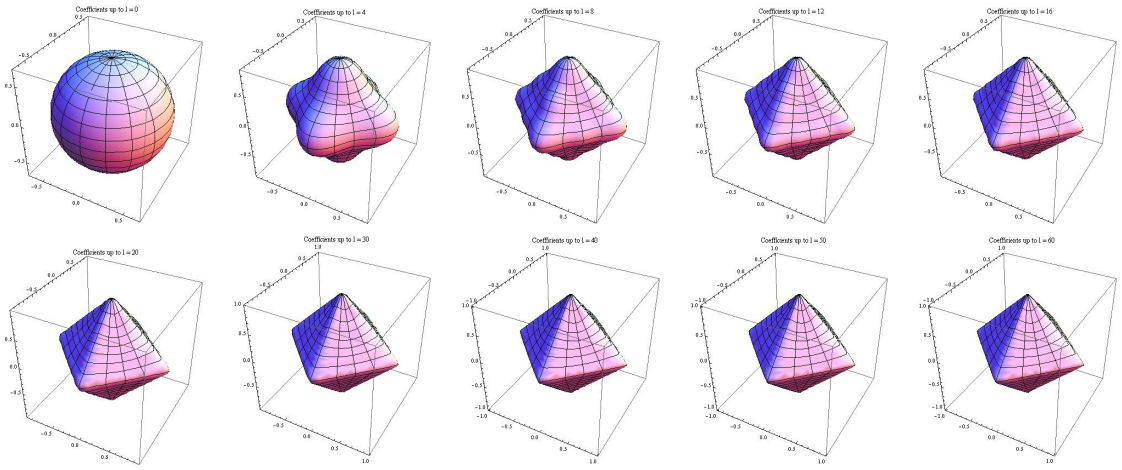

Figure 12: Approximation of the cross polytope as dual of the cube and its spherical harmonic expansion for coefficients up to $\ell = 0$, 4, 8, 12, 16, 20, 30, 40, 50, 60

The spherical harmonics Y_ℓ^m are in general nonconvex functions and so a linear combination of them is not likely to be a convex function. But for a function to be the support function of a convex body this function has to be convex. Therefore the finite spherical harmonic expansion of the cube does not correspond to a convex body, but it becomes close to it already for small ℓ. The family of convex bodies forms a cone, as described in section 2.1, and the cube lies in the boundary of this cone. When we take any point on the inside of any of the flat sides of the cube and flow this point inward an infinitesimal small distance the resulting body would no longer be convex. As a boundary body in the family of convex sets the cube is hence vulnerable to have a nonconvex expansion in spherical harmonics and the same argument is true for the cross polytope.

Having a visual idea about the approximation of the cube by its spherical harmonic expansion we now want to look at the Hausdorff and L^2 distance between the support function of the cube and its approximation. The results with respect to the summation index ℓ are presented in figure 13. Looking at the left graph corresponding to the Hausdorff distance, we see that the Hausdorff distance drops down and reaches

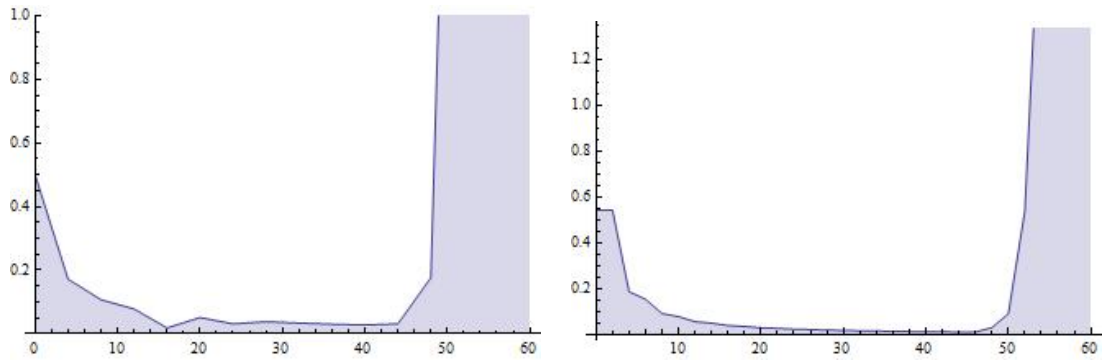

Figure 13: Distance between the cube and its spherical harmonic expansion with respect to the summation index ℓ - Left: Hausdorff distance, Right: L^2 distance

its minimum at $\ell = 16$ and then increases slightly and stays almost constant up to $\ell = 44$. After that the Hausdorff distances blows up and reaches values over 1000. The minimum obtained is 0.018 and after that the Hausdorff distance stays at about 0.03.

Compared to that, the L^2 distance, presented in the right graph, decreases monotonically until it blows up for $\ell > 46$. The minimum obtained is 0.009. The blow up is not as extreme as for the Hausdorff distance but it goes up to several hundreds as well.

We can conclude mainly two phenomena from this. First of all the L^2 distance seems to be more stable with regard to the numeric irregularities and nonconvex parts the finite spherical harmonic expansion has. The difference between the exact support function of the cube and its approximation are averaged out. In contrast the Hausdorff distance just takes into account the worst discrepancy between the exact and approximated support function and is hence more prone to numeric errors. The second phenomena is the blow up in both distances as the number of coefficients grows. Similar to the case where we plotted the bodies, it looks like the spherical harmonic expansion is too complicated to be handled and hence absurd results are produced.

Let us now look at the Mahler volume with respect to the summation index ℓ. To calculate it we use the basic formula in spherical coordinates (equation (46)) to calculate the volume of the dual body and the formula with the spherical Hessian (equation (67)) for the volume of the original body. Since the approximated support function is a smooth function, as a linear combination of smooth functions, the formula using the spherical Hessian can be applied successfully. The results of these calculations are summarized in Figure 14. With increasing ℓ the Mahler volume drops down, while

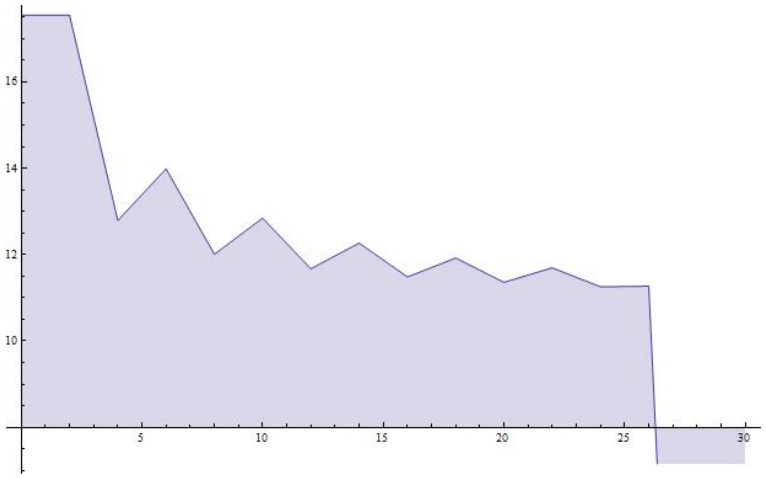

Figure 14: The Mahler volume of the spherical harmonic expansion of the cube with respect to the summation index ℓ

oscillating, to a value of 11.26 for $\ell = 26$. The Mahler volume of the cube in $\mathbb{R}^3$ is $8 \cdot \frac{4}{3} = 10\frac{2}{3}$, so the Mahler volume of the approximation is about 0.6 or 5.6% higher than the conjectured value. For $\ell \geq 28$ the results obtained are again compromised by numerical errors. The Mahler volume first drops down to a negative value and then stays at 0 for large ℓ.

5.4.2 Approximating the cross polytope by its spherical harmonic expansion

Now let us perform the same analysis for the approximation of the cross polytope. Whenever the results are similar to the approximation of the cube, the discussion

will be brief. For the cross polytope the coefficients have been calculated numerically in contrast to the exact coefficients of the cube. So there is an additional source for numerical errors by inexact coefficients c_l^m. The plots of the approximated cross polytope and its dual are summarized in Figures 15 and 16 for the values $\ell = 0$, 4, 8, 12, 16, 20, 30, 40, 50, 60.

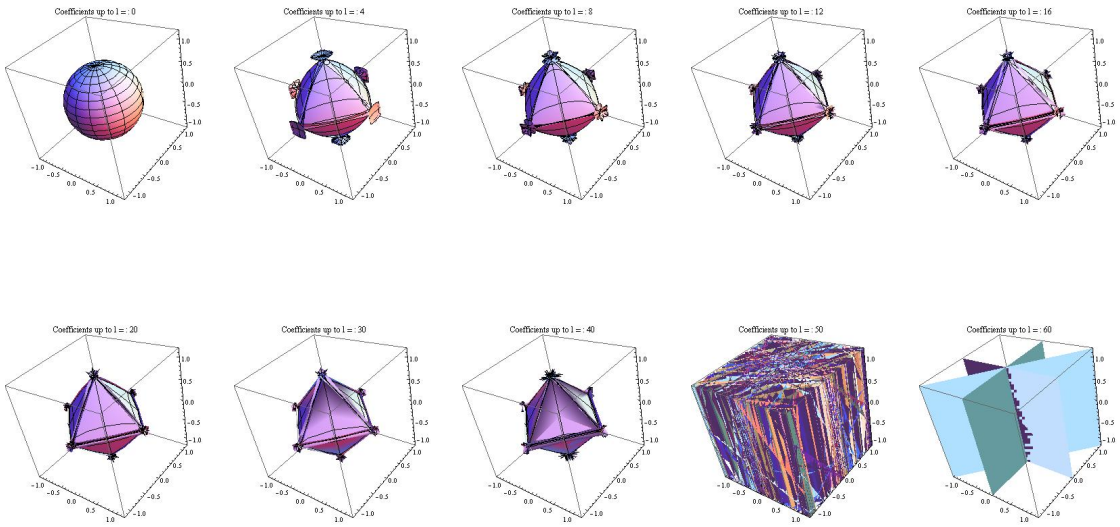

Figure 15: Approximation of the cross polytope by its spherical harmonic expansion for coefficients up to $\ell = 0$, 4, 8, 12, 16, 20, 30, 40, 50, 60

Looking at the visualizations of the approximated cross polytope we see similar results as for the cube. The flat sides overlap and are curved for small ℓ. As ℓ increases the flats straighten up and their overlaps become smaller. For $\ell = 20$ the approximation looks good again. The numeric errors in the coefficients do not seem to affect the approximation until $\ell = 40$. The only indicator of their errors is that already the approximation using coefficients up to $\ell = 50$ is a numeric artifact.
The dual body of this approximation behaves similarly to the dual body of the cube approximation. For small ℓ it has rounded corners and edges and dents on the flat sides which make the body nonconvex. Having a closer look at the body one can see

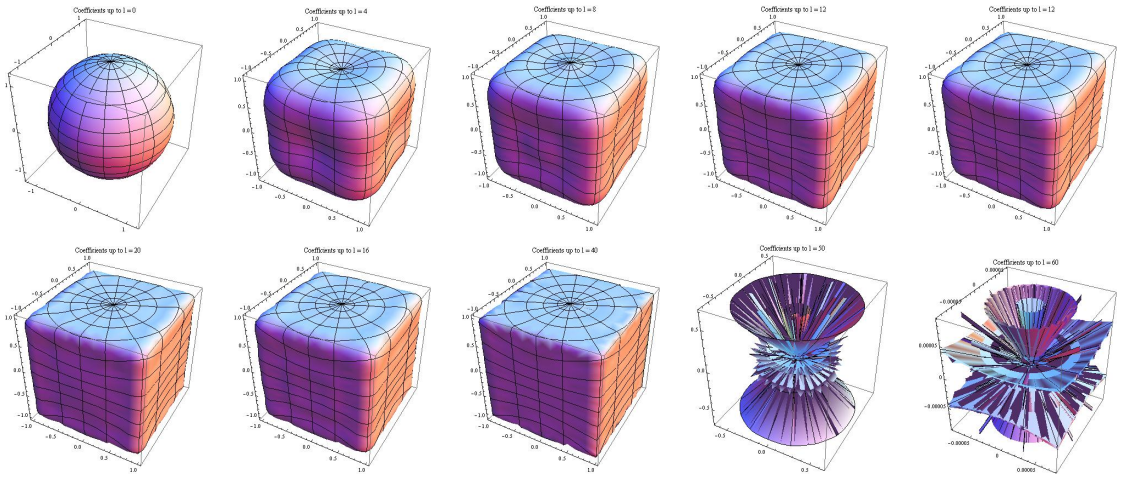

Figure 16: Approximation of the cube as dual of the cross polytope and its spherical harmonic expansion for coefficients up to $\ell = 0$, 4, 8, 12, 16, 20, 30, 40, 50, 60

that these rounded corners and dents in the flats stay up to $\ell = 30$. Just for $\ell = 40$ the corners look sharp and the flats straightened out. As for the original approximation we just get numerical artifacts when using coefficients up to $l = 50$.

Let us now look at the Hausdorff and L^2 distance between the cross polytope and its approximation with respect to the summation index ℓ. These results are summarized in Figure 17. The Hausdorff distances decreases as ℓ goes up until we get a blow up

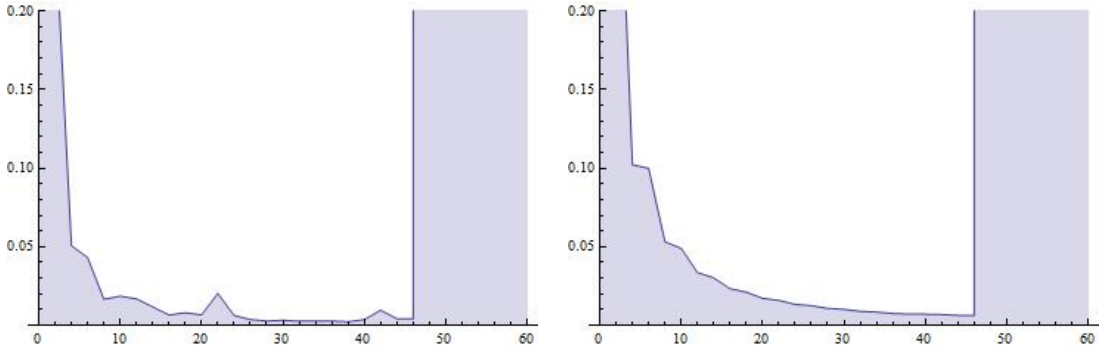

Figure 17: Distance between the cross polytope and its spherical harmonic expansion with respect to the summation index ℓ - Left: Hausdorff distance, Right: L^2 distance

at $\ell = 48$. The minimal value is obtained for $\ell = 38$ and is 0.0024. Similar to the approximation of the cube the decrease is not monotonic, and we observe bumps at $\ell = 10$, 18, 22 and 42.

The L^2 distances decreases monotonically again. It drops down to 0.0065 at $\ell = 44$. After that a blow up occurs. The L^2 distance seems to be more stable than the Hausdorff distance since it is able to average out numerical inaccuracies that just appear in small neighborhoods.

Finally let us look at the Mahler volume of the approximated cross polytope with respect to the summation index ℓ. The results are given in Figure 18 and this figure

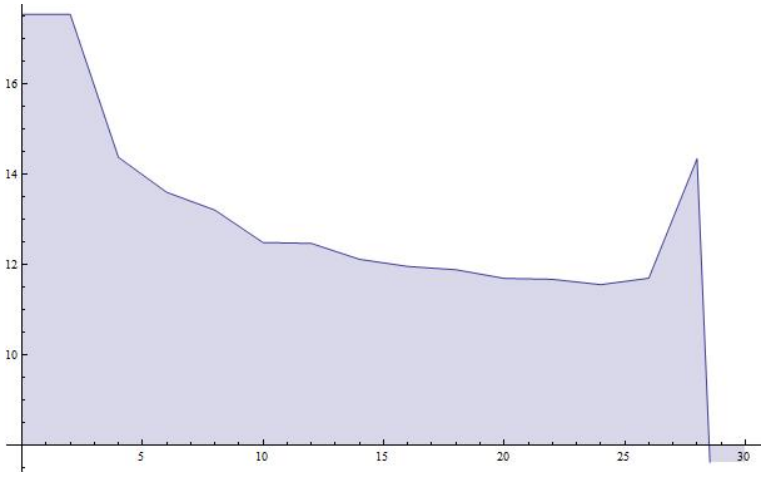

Figure 18: The Mahler volume of the spherical harmonic expansion of the cross polytope with respect to the summation index ℓ

shows that the Mahler volume decreases monotonically down to a value of 11.56 for $\ell = 24$ and then it increases for the next two approximations until it does not yield any more useful results for $\ell \geq 30$. So the approxmation of the cube produces slightly better results than the approximation of the cross polytope since the lowest Mahler volume calculated for the approximated cube is 11.26. Altogether the results for the two approximations are very similar.

5.5 Approximating the cube by approximating its radii of curvature

Another approach to approximate the cube is to approximate its radii of curvature. We know that the radii of curvature are related by the spherical Hessian and the Laplacian in spherical coordinates to the support functions by equations (60) and (61). Hence having the support function we can deduce a formula for the radii of curvature. For the cube we will see that these functions consist of Dirac δ functions. As the next step the Dirac δ functions, which are generalized functions, are approximated by ordinary functions. For that we use Gaussian functions with a small standard deviation and characteristic functions over a small interval. After replacing the Dirac δ functions with our approximations we can calculate the expansion of these functions in spherical harmonics. Using equation (75) we have the support function corresponding to the approximated radii of curvature. Now the volume product can be calculated using the basic formula in spherical coordinates for the volume of the dual body, equation (46), and the formula directly involving the radii of curvature, equation (66).

5.5.1 Deriving the radii of curvature for the cube and the cylinder

To derive the functions for the radii of curvature, we need to derive functions that involve absolute values. The absolute values can be rewritten using indicator or step functions $\mathcal{X}_S$, where S is a measurable set and they are defined as

$$\mathcal{X}_S(x) = \begin{cases} 1, & \text{for } x \in S \\ \\ 0, & \text{for } x \notin S \end{cases} .$$

Dirac δ functions can be seen as derivative of these step functions

$$\frac{d}{dx}\mathcal{X}_{(0,\,\infty)}(x) = \delta(x) \, . \tag{76}$$

In the language of the fundamental theorem of calculus this becomes

$$\int_{-\infty}^{x} \delta(a)\, da = \mathcal{X}_{(0,\,\infty)}(x)\ . \tag{77}$$

Properties of the Dirac δ function include

$$\delta(x-a) = 0 \quad \text{for } x \neq a\ . \tag{78}$$

In other terms it is zero everywhere except for the single point 0. This discussion prepares the formalism we need to deduce the radii of curvature.

Theorem 5.5.1 (The radii of curvature of the cube):

The mean and the product of the radii of curvature of the cube in spherical coordiantes are given by

$$\begin{aligned} &R_1(\theta,\varphi) + R_2(\theta,\varphi) = \\ &\qquad = 2\delta\big(\theta - \frac{\pi}{2}\big) + \frac{2}{\sin(\theta)}\Big[\delta\big(\varphi\big) + \delta\big(\varphi - \frac{\pi}{2}\big) + \delta\big(\varphi - \pi\big) + \delta\big(\varphi - \frac{3}{2}\pi\big)\Big] \end{aligned} \tag{79}$$

and

$$\begin{aligned} &R_1(\theta,\varphi) \cdot R_2(\theta,\varphi) = \\ &\qquad = 2\delta\big(\theta - \frac{\pi}{2}\big) \cdot \frac{2}{\sin(\theta)}\Big[\delta\big(\varphi\big) + \delta\big(\varphi - \frac{\pi}{2}\big) + \delta\big(\varphi - \pi\big) + \delta\big(\varphi - \frac{3}{2}\pi\big)\Big]\ . \end{aligned} \tag{80}$$

Proof. Recall the support function of the cube as given in equation (12). In spherical coordinates it becomes

$$h(\theta,\varphi) = |\cos(\varphi)\sin(\theta)| + |\sin(\varphi)\sin(\theta)| + |\cos(\theta)|\ . \tag{81}$$

We will replace the absolute values by multiplying the functions with characteristic functions that mirror the change of the sign of the functions. These characteristic functions will depend on the angle with respect to which we derive. Note that $\varphi \in [0, 2\pi)$ can be thought of as a periodic angle, but not $\theta \in [0, \pi]$. As a consequence $|\sin(\theta)| = \sin(\theta)$, but $|\sin(\varphi)| = \sin(\varphi)(2\mathcal{X}_{(0,\,\pi]}(\varphi) - 1)$ has a characteristic functions

with two jump points, namely $\varphi = 0$ and $\varphi = \pi$.

We calculate, step by step, the Hessian and the Laplacian in spherical coordinates, as given in equations (60) and (61), of this support function. Let us start the book-keeping. First calculate the derivatives with respect to θ:

$$\begin{aligned}
\frac{\partial}{\partial\theta}|\cos(\varphi)\sin(\theta)| &= \frac{\partial}{\partial\theta}|\cos(\varphi)|\sin(\theta) = |\cos(\varphi)|\cos(\theta) \\
\frac{\partial^2}{\partial\theta^2}|\cos(\varphi)\sin(\theta)| &= -|\cos(\varphi)|\sin(\theta)
\end{aligned}$$

$$\begin{aligned}
\frac{\partial}{\partial\theta}|\sin(\varphi)\sin(\theta)| &= \frac{\partial}{\partial\theta}|\sin(\varphi)|\sin(\theta) = |\sin(\varphi)|\cos(\varphi) \\
\frac{\partial^2}{\partial\theta^2}|\sin(\varphi)\sin(\theta)| &= -|\sin(\varphi)|\sin(\theta)
\end{aligned}$$

$$\begin{aligned}
\frac{\partial}{\partial\theta}|\cos(\theta)| &= \frac{\partial}{\partial\theta}\cos(\theta)\big(2\mathcal{X}_{[0,\,\pi/2]}(\theta) - 1\big) = \\
&= -\sin(\theta)\big(2\mathcal{X}_{[0,\,\pi/2]}(\theta) - 1\big) + \cos(\theta)\big(-2\delta(\theta - \pi/2)\big) = \\
&= -\sin(\theta)\big(2\mathcal{X}_{[0,\,\pi/2]}(\theta) - 1\big)\ , \quad \text{as } \cos(\pi/2) = 0\ . \\
\frac{\partial^2}{\partial\theta^2}|\cos(\theta)| &= -\cos(\theta)\big(2\mathcal{X}_{[0,\,\pi/2]}(\theta) - 1\big) - \sin(\theta)\big(-2\delta(\theta - \pi/2)\big) = \\
&= -|\cos(\theta)| + 2\delta(\theta - \pi/2)
\end{aligned}$$

We then calculate the derivatives with respect to φ:

$$\begin{aligned}
\frac{\partial}{\partial\varphi}|\cos(\varphi)\sin(\theta)| &= \frac{\partial}{\partial\varphi}\cos(\varphi)\big(2\mathcal{X}_{(0,\,\pi/2]}(\varphi)+2\mathcal{X}_{(3\pi/2,\,2\pi]}(\varphi)-1\big)\sin(\theta) = \\
&= -\sin(\varphi)\big(2\mathcal{X}_{(0,\,\pi/2]}(\varphi)+2\mathcal{X}_{(3\pi/2,\,2\pi]}(\varphi)-1\big)\sin(\theta)+ \\
&\quad +\cos(\varphi)\big(-2\delta(\varphi-\pi/2)+2\delta(\varphi-3\pi/2)\big)\sin(\theta) = \\
&= -\sin(\varphi)\big(2\mathcal{X}_{(0,\,\pi/2]}(\varphi)+2\mathcal{X}_{(3\pi/2,\,2\pi]}(\varphi)-1\big)\sin(\theta) \\
\frac{\partial^2}{\partial\varphi^2}|\cos(\varphi)\sin(\theta)| &= -\cos(\varphi)\big(2\mathcal{X}_{(0,\,\pi/2]}(\varphi)+2\mathcal{X}_{(3\pi/2,\,2\pi]}(\varphi)-1\big)\sin(\theta)- \\
&\quad -\sin(\varphi)\big(-2\delta(\varphi-\pi/2)+2\delta(\varphi-3\pi/2)\big)\sin(\theta) = \\
&= -|cos(\varphi)|\sin(\theta)+\big(2\delta(\varphi-\pi/2)+2\delta(\varphi-3\pi/2)\big)\sin(\theta)
\end{aligned}$$

$$\begin{aligned}
\frac{\partial}{\partial\varphi}|\sin(\varphi)\sin(\theta)| &= \frac{\partial}{\partial\varphi}\sin(\varphi)\big(2\mathcal{X}_{(0,\,\pi]}(\varphi)-1\big)\sin(\theta) = \\
&= \cos(\varphi)\big(2\mathcal{X}_{(0,\,\pi]}(\varphi)-1\big)\sin(\theta)+ \\
&\quad +\sin(\varphi)\big(2\delta(\varphi)-2\delta(\varphi-\pi)\big)\sin(\theta) = \\
&= \cos(\varphi)(2\mathcal{X}_{(0,\,\pi]}(\varphi)-1)\sin(\theta) \\
\frac{\partial^2}{\partial\varphi^2}|\sin(\varphi)\sin(\theta)| &= -\sin(\varphi)\big(2\mathcal{X}_{(0,\,\pi]}(\varphi)-1\big)\sin(\theta)+ \\
&\quad +\cos(\varphi)\big(2\delta(\varphi)-2\delta(\varphi-\pi)\big)\sin(\theta) = \\
&= -|\sin(\varphi)|\sin(\theta)+\big(2\delta(\varphi)+2\delta(\varphi-\pi)\big)\sin(\theta)
\end{aligned}$$

$$\begin{aligned}
\frac{\partial}{\partial\varphi}|cos(\theta)| &= 0 \\
\frac{\partial^2}{\partial\varphi^2}|cos(\theta)| &= 0
\end{aligned}$$

Now let us plug these into the formula for the Laplacian in spherical coordinates.

First calculate $\big(\frac{\partial^2}{\partial\theta^2}+1\big)h$ and then $\big(\frac{\cos(\theta)}{\sin(\theta)}\frac{\partial}{\partial\theta}+\frac{1}{\sin^2(\theta)}\frac{\partial^2}{\partial\varphi^2}+1\big)h$:

$$\begin{aligned}\left(\frac{\partial^2}{\partial\theta^2}+1\right)h(\theta,\varphi) &= \\ &= -|\cos(\varphi)|\sin(\theta)-|\sin(\varphi)|\sin(\theta)-|\cos(\theta)|+2\delta(\theta-\pi/2)+ \\ &\quad +|\cos(\varphi)|\sin(\theta)+|\sin(\varphi)|\sin(\varphi)+|\cos(\theta)|= \\ &= 2\delta(\theta-\pi/2)\end{aligned}$$

$$\begin{aligned}\left(\frac{\cos(\theta)}{\sin(\theta)}\frac{\partial}{\partial\theta}+\frac{1}{\sin^2(\theta)}\frac{\partial^2}{\partial\varphi^2}+1\right)h(\theta,\varphi) &= \\ &= \frac{\cos(\theta)}{\sin(\theta)}\Big[|\cos(\varphi)|\cos(\theta)+|sin(\varphi)|\cos(\varphi)-\sin(\theta)\big(2\mathcal{X}_{[0,\,\pi/2]}(\theta)-1\big)\Big]+ \\ &\quad +\frac{1}{\sin^2(\theta)}\Big[-|cos(\varphi)|\sin(\theta)+\big(2\delta(\varphi-\pi/2)+2\delta(\varphi-3\pi/2)\big)\sin(\theta)- \\ &\quad -|\sin(\varphi)|\sin(\theta)+\big(2\delta(\varphi)+2\delta(\varphi-\pi)\big)\sin(\theta)+0\Big]+ \\ &\quad +|\cos(\varphi)|\sin(\theta)+|sin(\varphi)|\sin(\varphi)+|\cos(\theta)|= \\ &= \left[(1-\sin^2(\theta))\Big(\frac{|\cos(\varphi)|}{\sin(\theta)}+\frac{|\sin(\varphi)|}{\sin(\theta)}\Big)+\cos(\theta)\big(2\mathcal{X}_{[0,\,\pi/2]}(\theta)-1\big)\right]+ \\ &\quad +\Big[\frac{1}{\sin(\theta)}\big(-|\cos(\varphi)|-|\sin(\varphi)| \\ &\quad +2\delta(\varphi-\pi/2)+2\delta(\varphi-3\pi/2)+2\delta(\varphi)+2\delta(\varphi-\pi)\big)\Big]+ \\ &\quad +|\cos(\varphi)|\sin(\theta)+|sin(\varphi)|\sin(\varphi)+|\cos(\theta)|= \\ &= \frac{2}{\sin(\theta)}\big(\delta(\varphi)+\delta(\varphi-\pi/2)+\delta(\varphi-\pi)+\delta(\varphi-3\pi/2)\big)\end{aligned}$$

So finally we get by equation (61)

$$R_1(\theta,\varphi)+R_2(\theta,\varphi)=2\delta(\theta-\pi/2)+\frac{2}{\sin(\theta)}\big(\delta(\varphi)+\delta(\varphi-\pi/2)+\delta(\varphi-\pi)+\delta(\varphi-3\pi/2)\big)\ .$$

For the Hessian in spherical coordinates we need to calculate mixed derivatives:

$$\frac{\partial}{\partial\theta}\frac{1}{\sin(\theta)}\frac{\partial}{\partial\varphi}|\cos(\varphi)\sin(\theta)| =$$
$$= \frac{\partial}{\partial\theta}\frac{1}{\sin(\theta)}\Big(-\sin(\varphi)\big(2\mathcal{X}_{(0,\,\pi/2]}(\varphi)+2\mathcal{X}_{(3\pi/2,\,2\pi]}(\varphi)-1\big)\sin(\theta)\Big) = 0$$

$$\frac{\partial}{\partial\theta}\frac{1}{\sin(\theta)}\frac{\partial}{\partial\varphi}|\sin(\varphi)\sin(\theta)| = \frac{\partial}{\partial\theta}\frac{1}{\sin(\theta)}\cos(\varphi)\big(2\mathcal{X}_{(0,\,\pi]}(\varphi)-1\big)\sin(\theta) = 0$$

$$\frac{\partial}{\partial\theta}\frac{1}{\sin(\theta)}\frac{\partial}{\partial\varphi}|\cos(\theta)| = 0$$

So we get $\frac{\partial}{\partial\theta}\frac{1}{\sin(\theta)}\frac{\partial}{\partial\varphi}h(\theta,\varphi) = 0$ and hence by equation (60)

$$R_1(\theta,\varphi)\cdot R_2(\theta,\varphi) = \big(2\delta(\theta-\pi/2)\big)\cdot\frac{2}{\sin(\theta)}\Big[\delta(\varphi)+\delta(\varphi-\pi/2)+\delta(\varphi-\pi)+\delta(\varphi-3\pi/2)\Big]\,.$$

□

Theorem 5.5.2 (The radii of curvature of the cylinder):

The mean and the product of the principal radii of curvature of the cylinder are given by

$$R_1(\theta,\varphi)+R_2(\theta,\varphi) = 2\delta(\theta-\pi/2)+\frac{1}{\sin(\theta)} \quad \text{and} \tag{82}$$
$$R_1(\theta,\varphi)\cdot R_2(\theta,\varphi) = 2\delta(\theta-\pi/2)\cdot\frac{1}{\sin(\theta)}\,. \tag{83}$$

Proof. The proof will be similar to the derivation of the mean and product of the principal radii of curvature for the cube. Let us first recall the support function of the cylinder as given in equation (17). In spherical coordinates it becomes

$$h(\theta,\varphi) = \sin(\theta)+|\cos(\theta)|\,. \tag{84}$$

Again, let us start the bookkeeping. First calculate the derivatives with respect to θ:

$$\begin{aligned}
\frac{\partial}{\partial\theta}\Big(\sin(\theta)+|\cos(\theta)|\Big) &= \frac{\partial}{\partial\theta}\sin(\theta)+\cos(\theta)\big(2\mathcal{X}_{[0,\,\pi/2)}(\theta)-1\big)= \\
&= \cos(\theta)-\sin(\theta)\big(2\mathcal{X}_{[0,\,\pi/2)}(\theta)-1\big)+ \\
&\quad +\cos(\theta)\big(-2\delta(\theta-\pi/2)\big)= \\
&= \cos(\theta)-\sin(\theta)\big(2\mathcal{X}_{[0,\,\pi/2)}(\theta)-1\big) \\
\frac{\partial^2}{\partial\theta^2}\Big(\sin(\theta)+|\cos(\theta)|\Big) &= -\sin(\theta)-\cos(\theta)\big(2\mathcal{X}_{[0,\,\pi/2)}(\theta)-1\big)- \\
&\quad -\sin(\theta)\big(-2\delta(\theta-\pi/2)\big)= \\
&= -\sin(\theta)-|\cos(\theta)|+2\delta(\theta-\pi/2)
\end{aligned}$$

Since the body is rotationally symmetric with respect to the x_3-axis, the support function is independent of φ, and hence all derivatives with respect to φ, including the mixed derivatives, are 0.

So let us calculate the spherical Laplacian (61) to get

$$\begin{aligned}
R_1(\theta,\varphi)+R_2(\theta,\varphi) &= \Big(\frac{\partial^2}{\partial\theta^2}+\frac{\cos(\theta)}{\sin(\theta)}\frac{\partial}{\partial\theta}+\frac{1}{\sin^2(\theta)}\frac{\partial^2}{\partial\varphi^2}+2\Big)h(\theta,\varphi)= \\
&= -\sin(\theta)-|\cos(\theta)|+2\delta(\theta-\pi/2)+ \\
&\quad +\frac{\cos(\theta}{\sin(\theta)}\Big[\cos(\theta)-\sin(\theta)\big(2\mathcal{X}_{[0,\,\pi/2)}(\theta)-1\big)\Big]+ \\
&\quad +0+2\big[sin(\theta)+|\cos(\theta)|\big]= \\
&= 2\delta(\theta-\pi/2)+\frac{1-\sin^2(\theta)}{\sin(\theta)}-|\cos(\theta)|+sin(\theta)+|\cos(\theta)|= \\
&= 2\delta(\theta-\pi/2)+\frac{1}{\sin(\theta)}\,.
\end{aligned}$$

Similarly we get for the Hessian in spherical coordinates, as given in equation (60),

$$\begin{aligned}
R_1(\theta,\varphi)\cdot R_2(\theta,\varphi) = \Big[\Big(\Big(\frac{\partial^2}{\partial\theta^2}+1\Big)h(\theta,\varphi)\Big)\cdot \\
\cdot\Big(\Big(\frac{\cos(\theta)}{\sin(\theta)}\frac{\partial}{\partial\theta}+\frac{1}{\sin^2(\theta)}\frac{\partial^2}{\partial\varphi^2}+1\Big)h(\theta,\varphi)\Big)\Big]- \\
-\Big[\Big(\frac{\partial}{\partial\theta}\frac{1}{\sin(\theta)}\frac{\partial}{\partial\varphi}\Big)h(\theta,\varphi)\Big]^2 = \\
=\Big(-\sin(\theta)-|\cos(\theta)|+2\delta(\theta-\pi/2)+sin(\theta)+|\cos(\theta)|\Big)\cdot \\
\cdot\Big(\frac{\cos(\theta}{\sin(\theta)}\big[\cos(\theta)-\sin(\theta)\big(2\mathcal{X}_{[0,\,\pi/2)}(\theta)-1\big)\big]+ \\
+\sin(\theta)+|\cos(\theta)|\Big)-0= \\
=2\delta(\theta-\pi/2)\cdot\frac{1}{\sin(\theta)};.
\end{aligned}$$

□

5.5.2 Approximating the radii of curvature of the cube

Given the sum of the radii of curvature of the cube, as in equation (79), we see that it consists of Dirac δ functions. These are now approximated. First we use Gaussians given by $\frac{1}{\sigma\sqrt{2\pi}}e^{-\frac{(x-\mu_0)^2}{2\sigma^2}}$ with mean μ and standard deviation σ. For each Gaussian we set the mean to the point were the blow-up of the corresponding Dirac δ function occurs. For $\delta(\varphi)$ we use that φ is a periodic angle and let the corresponding Gaussian decay on both sides of the interval $[0, 2\pi)$. The standard deviation σ is set to a small value so that the peak of the Gaussian is high and it decays fast.

Calculating the spherical harmonics coefficients of the sum of the radii of curvature yields that they have same structure as the coefficients of the support function of the cube, which were given in Table 4. Equation (75) relates all coefficients for $\ell \neq 1$ of the mean curvature to the coefficients of the support function. The coefficients c_1^m for $m = -1,\, 0,\, 1$ are determined by the so called Steiner point. If this point is at the origin, these coefficients are 0. As we have seen in the expansion of the support function of the cube, its Steiner point is at the origin. The coefficients of the sum of

the radii of curvature corresponding to $\ell = 1$ are 0 as well, so this poses no problem. First, let us again have a look at the bodies created in that way. The approximated

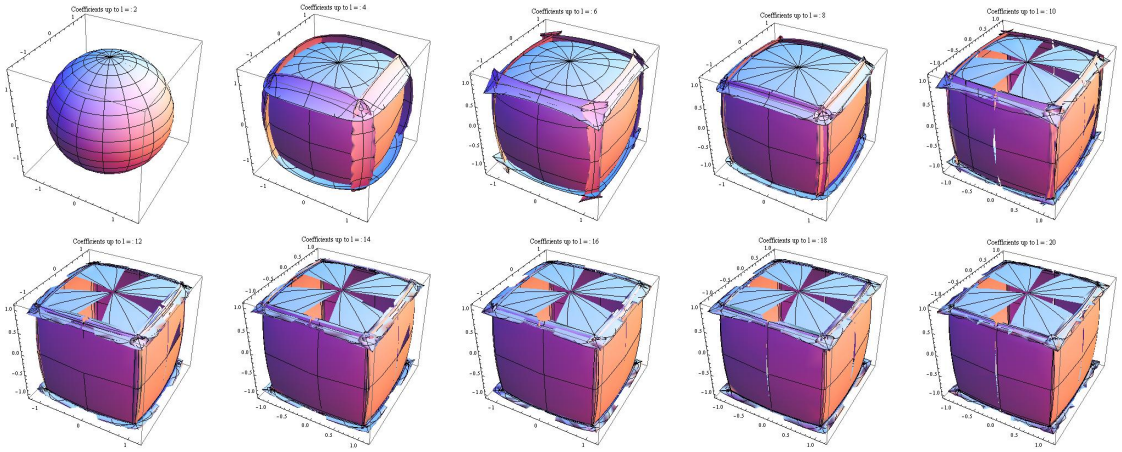

Figure 19: Approximation of the cube by approximating its radii of curvature for $\ell = 2, 4, 6, 8, 10, 12, 14, 16, 18, 20$

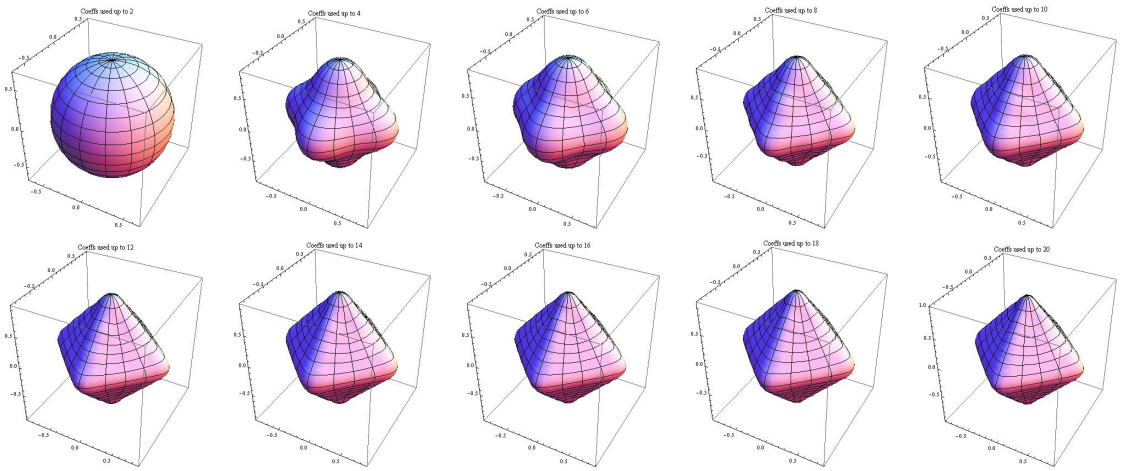

Figure 20: Approximation of the cross polytope as dual body of the cube with approximated radii of curvature for $\ell = 2, 4, 6, 8, 10, 12, 14, 16, 18, 20$

body and its dual are presented in Figures 19 and 20 for different values of the summaton index ℓ, respectively. Here $\sigma = 0.1$ was choosen for the Gaussians.

Looking at the plots, the approximated cube looks similar to the direct approximation

of the cube support function in spherical harmonics. The same overlap of the flats occur. These flats are bend for small ℓ but this bending decreases as ℓ increases. The overlap of the flats decreases as well for larger ℓ. From $\ell = 10$ on we observe that the approximation of the cube looks like it is sliced along the $x-$ and $y-$axes on the top face. For $\ell = 18$ and 20 this slicing continues down the sides.

The dual body also behaves similarly to the dual body of the support function approximation. For small ℓ it looks nonconvex at the flats and the edges but it has rounded corners. As ℓ increases the nonconvex parts become straight and the edges and corners become sharp.

Altogether the bodies look very similar to the first set of experiments, where the support function of the body was approximated. But calculating their Mahler volume yields an interesting result. The calculated values for the volume product are given in Figure 21 for ℓ up to 50. Blue are the values calculated for the approximation of the cube and the red and yellow lines indicate the volume product of the cube and the ball respectively. The volume product is first oscillating and then seems to converge.

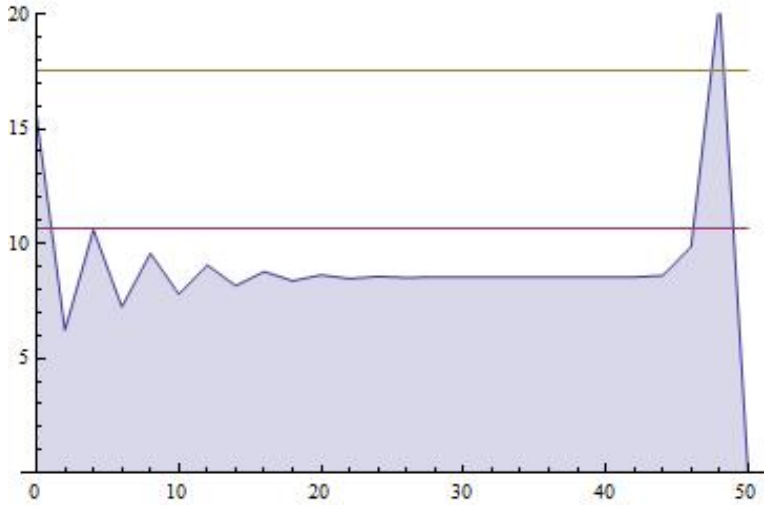

Figure 21: The Mahler volume of the body generated by approximating the radii of curvature of the cube with respect to the summation index ℓ of the expansion

It stays almost constant at about 8.5 unti $\ell = 42$. It then blows up over 20, which is

more than the proved upper bound for the volume product, and finally drops down to 0 for $\ell = 50$. The blow up and decay to 0 are concluded to be numerical errors. For the direct approximation of the cube and the cross polytope the numerical errors started to appear for similar ℓ. But for small ℓ the volume product of the approximations is smaller than the conjectured value. That the volume product is not just slightly smaller but several units below the Mahler volume even for large ℓ is very interesting. This means that we can create bodies, that are close, for example in the L^2 sense, to the cube but they have a significant smaller volume product. In the limit, as ℓ goes to infinity, the bodies would actually become convex. If the volume product stays at the value to which it seems to converge for small ℓ, this body would contradict Mahler's conjecture. Nevertheless we are not able to verify this, since the calculations encounter numerical problems for $\ell > 42$. That the bodies are nonconvex is verified by a closer look at the radii of curvature. Both take negative values and hence the body cannot be convex. This phenomenon appears for all ℓ up to 50 and the lowest value the radii of curvature take stays somewhere near -2.

That the radii of curvature are negative and hence the bodies not convex has drastic impacts on the experiments. Formula (68) to visualize the original body is just valid for convex bodies and so is equation (69) to visualize the dual. Furthermore the support is defined only for convex bodies and the formulas used to calculate the volume product involve these formulas as well as they require convexity of the body. Nevertheless Figure 19 suggests that the volume product of the approximation is converging to some value smaller than the conjectured minimal Mahler volume. Having the Gaussians as approximations of the Dirac δ functions and not their approximation in spherical harmonics, the radii of curvature have to be positive, since we just add positive quantities. Hence the resulting body is very likely to be convex, and if the volume product of the approximations is converging to some number, it should be the volume product of that body. So this body, having Gaussians instead of Dirac δ

functions in the radii of curvature, would be very interesting to examine. But without the spherical harmonics we have no tool to examine it, since we are missing the link to the support function.

Besides this one experiment where σ was set to 0.1, experiments with different values for the standard deviation, namely 0.05 and 0.01 were run. The results are very similar. The Mahler volume of the approximation looks like it converges to some number smaller than the conjectured value and it is smaller for smaller σ. The radii of curvature are negative for any size of the summation, except for the trivial case $\ell = 0$.

Experiments with characteristic functions over a small set of support instead of Gaussians as approximations of the Dirac δ functions were run as well. The results concerning the Mahler volume and the radii of curvature are similar.

To show that the issues we encounter with this approximation are not because of Mahler's conjecture and the problem itself but a weakness of the approach used, the cylinder and its support function are approximated in the same way. The Mahler volume of this approximation shows the same oscillating behavior and the values taken are several units below the volume product of the cube. The radii of curvature are again negative which explains the lower value calculated with the volume product. As the cylinder is known not to be a candidate to minimize the Mahler volume, its volume product is $\frac{4}{3}\pi^2 \approx 13.16 > 10\frac{2}{3}$, this shows that we have to be very careful when calculating the spherical harmonic expansion of the approximate delta functions. It is easily the case that this expansion makes the radii of curvature negative and the body nonconvex. And furthermore this shows that the problems we encounter are not directly related to the problem we want to solve, but to the method used. Although that may be a good result it also shows the small volume product we encounter for the approximations of the cube may not be related to a body who is actually a counterexample to Mahler's conjecture. The approximations

of the cylinder are not likely to have a smaller volume product than the cube, since the volume product of the cylinder is almost 2 units bigger than that of the cube. Hence the small volume products we encounter for both approximations, of the cube and the cylinder, are likely to be related to the used methods as well. Nevertheless it may be worthwhile to derive the support function of the cube with Gaussians instead of Dirac δ to check the results encountered.

Let us conclude this chapter with a short discussion about why the radii of curvature take negative values. The approximate delta functions take very small values almost everywhere until they shoot up at certain points. To capture this rapid increase and the maximum value taken by the approximate deltas a finite approximation in spherical harmonics has to decrease below the actual value of the approximate delta before and after the blow up. As these values are already close to 0 the finite expansion is likely to overshoot and to take a negative value and hence the resulting body will no longer be convex. There are mainly two ways to resolve this problem: One could either use a spherical harmonic expansion up to a very high order or set some threshold below the approximate deltas are not allowed to drop. The first attempt will encounter numerical problems as the spherical harmonics oscillate highly as their indices grow. The second approach will result in a rounder body, which is less like to beat the cube in terms of the volume product. The best way would be to stay with the approximated delta functions, e.g. Gaussians, directly but this hides the support function of the body, which is necessary for the volume product calculations. Using a different orthonormal basis as the spherical harmonics does not solve the problem of overshooting and negative radii of curvature. Any complete orthonormal set will encounter this problem for sufficiently small σ.

CHAPTER VI

CONCLUSIONS

For smooth convex bodies in $\mathbb{R}^3$ we showed an efficient way to calculate the Mahler volume using the Hessian in spherical coordiantes. Having the support function makes it easier to calculate the volume of the dual body and the formula for the dual volume also applies efficiently in the nonconvex case and to higher dimensions.

The volume of the original body is harder to calculate but the Legendre transform in Cartesian coordinates relates the support function with the gauge function of the body. Therefore we can use it to calculate the volume of the body if it is nonconvex and in arbitrary dimensions. Although this gives a general formula, the experiments have shown, that this approach is not efficient, even in 3 dimensions. Each time the Legendre transform is evaluated, a maximization is performed. To do that, we used a standard maximization algorithm taking no advantage of the special structure of the problem. We know, for example, that the support function is convex, which makes the maximization problem much easier to solve.

Furthermore we can use the structure of the Legendre transform to speed up its calculation instead of using a generic maximization algorithm. In [14] a linear time algorithm to compute the Legendre transform is introduced. It could be exploited to speed up the computations making the formula using the Legendre transform suitable to calculate the volume of a convex body in the nonsmooth case and for arbitrary dimensions. If the improvement in terms of running time is high enough, this would yield an efficient way to calculate the Mahler volume for all convex body in all dimensions.

Approximating the conjectured minimizers of the volume product by their spherical

harmonic expansion encountered several difficulties. The bodies created are nonconvex and the volume product calculated stays several percent above the conjectured minimum. We have seen that numerical calculations involving spherical harmonics are not stable if the expansion gets too large. While plotting the bodies and calculating their distances yielded good results up to $\ell \geq 40$, calculating the Mahler volume encountered problems earlier, below $\ell = 30$. When comparing the approximation of the cube and the cross polytope with the original bodies, we have seen that the L^2 distance more suitable for this purpose than the Hausdorff distance. It is more stable in terms of numerical errors in the support functions which appear in a large spherical harmonic expansion, as it averages them out.

The final set of experiments showed interesting results. Approximating the radii of curvature of the cube by Gaussians suggested that a body created in that way may have smaller volume product than the cube. As we were only able to approximate these Gaussians by their spherical harmonics expansion, the radii of curvature always take negative values, and hence the resulting bodies are nonconvex. The problem is to deduce the support function of the body having the radii of curvature. Without using spherical harmonics the support function is given as a solution to partial differential equations using the Hessian or Laplacian in spherical coordinates. In our case these partial differential equations become

$$2h(\theta,\varphi)\frac{\partial^2}{\partial\theta^2}h(\theta,\varphi) + \frac{\cos(\theta)}{\sin(\theta)}\frac{\partial}{\partial\theta}h(\theta,\varphi) + \frac{1}{\sin^2(\theta)}\frac{\partial^2}{\partial\varphi^2}h(\theta,\varphi) - \\ - \frac{2}{\sigma\sqrt{2\pi}}\left(e^{-\frac{(\theta-\pi/2)^2}{2\sigma^2}} + \frac{1}{\sin(\theta)}\left(e^{-\frac{(\varphi)^2}{2\sigma^2}} + e^{-\frac{(\varphi-\pi/2)^2}{2\sigma^2}} + e^{-\frac{(\varphi-\pi)^2}{2\sigma^2}} + e^{-\frac{(\varphi-3\pi/2)^2}{2\sigma^2}}\right)\right) = 0 \tag{85}$$

and

$$\Big(\Big(\frac{\partial^2}{\partial\theta^2}h(\theta,\varphi)+h(\theta,\varphi)\Big)\cdot\Big(\frac{\cos(\theta)}{\sin(\theta)}\frac{\partial}{\partial\theta}h(\theta,\varphi)+\frac{1}{\sin^2(\theta)}\frac{\partial^2}{\partial\varphi^2}h(\theta,\varphi)+h(\theta,\varphi)\Big)\Big)- \\ -\Big(\frac{\partial}{\partial\theta}\frac{1}{\sin(\theta)}\frac{\partial}{\partial\varphi}h(\theta,\varphi)\Big)^2- \\ -\frac{4e^{-\frac{(\theta-\pi/2)^2}{2\sigma^2}}}{\sigma^2\pi\sin(\theta)}\Big(e^{-\frac{(\varphi)^2}{2\sigma^2}}+e^{-\frac{(\varphi-\pi/2)^2}{2\sigma^2}}+e^{-\frac{(\varphi-\pi)^2}{2\sigma^2}}+e^{-\frac{(\varphi-3\pi/2)^2}{2\sigma^2}}\Big)=0 \tag{86}$$

for some $\sigma > 0$ and Dirichlet boundary conditions. Since scaling of the body does not matter we can set $h(0,0) = 1$. We then get $h(0,\pi) = h(0,0)$ by symmetry of the body and $h(2\pi,0) = h(0,0)$ and $h(2\pi,\pi) = h(0,\pi)$ by periodicity of the angle φ. The same approximation of the cylinder, whose support function would be given by similar partial differential equations, also results in a smaller calculated volume product. Since the cylinder is not a candidate to minimize the Mahler volume, this makes the cube with Gaussians in the radii of curvature less likely to have smaller volume product than the cube. Nevertheless, the partial differential equation given by equation (85) looks worth trying to derive the support function of the approximated cube. One could either try to find a closed form for the solution or solve this partial differential equation with numerical methods.

APPENDIX A

MATHEMATICA NOTEBOOK: MAHLER VOLUME COMPUTATIONS

REFERENCES

[1] Abramowitz, M. and Stegun, I., *Handbook of Mathematical Functions with Formulas, Graphs and Mathematical Tables*. US Department of Commerce, 1964.

[2] Arnold, V., *Geometrical Methods in the Theory of Ordinary Differential Equations*. Springer Verlag, 1988.

[3] Blaschke, W., "Ueber affine geometrie vii: Neue extremeiegenschaften von ellipse und ellipsoid," *Leipziger Ber.*, vol. 69, pp. 306–318, 1917.

[4] Blaschke, W., *Vorlesungen ueber Differentialgeometrie II.* Springer Wien, 1923.

[5] Bourgain, J. and Milman, V., "New volume ratio properties for convex symmetric bodies in $\mathbb{R}^n$," *Invent. Math*, vol. 88, pp. 319–340, 1987.

[6] Evans, L. C., *Partial Differential equations*. American Mathematical Society, 1998.

[7] Giaquinta, M. and Hildebrandt, S., *Calculus of Variations II*. Springer Verlag, 1996.

[8] Gordon, Y., Meyer, M., and Reisner, S., "Zonoids with minimal volume-product - a new proof," *Proceedings of the american mathematical society*, vol. 104, nr. 1, 1988.

[9] Groemer, H., *Geometric Applications of Fourier Series and Spherical Harmonics*. Cambridge University Press, 1996.

[10] Hadwiger, H., *Altes und neues ueber konvexe Koerper*. Birkhaeuser Verlag, 1955.

[11] John, F., "Extremum problems with inequalities as subsidiary conditions," *Studies and essays presented to R. Courant on his 60th birthday, Interscience Publishers Inc., New York (Jan. 8 1948)*, vol. 52, pp. 187–204, 1948.

[12] Kuperberg, G., "A low-technology estimate in convex geometry," *Internat. Math. Res. Notices*, vol. 9, pp. 181–183, 992.

[13] Kuperberg, G., "From the mahler conjecture to gauss linking integrals," 2006.

[14] Lucet, Y., "Faster than the fast legendre transform, the linear-time legendre transform," *Numerical Algorithms*, vol. 16, pp. 171–185, 1997.

[15] Mahler, K., "Ein minimalproblem fuer konvexe polygone," *Mathematica (Zutphen)*, vol. B 7, pp. 118–127, 1939.

[16] Mahler, K., "Ein uebertragungsprinzip fuer konvexe koerper," *Casopis pro pestovani a fysiky*, vol. 68, no. 3, pp. 93–102, 1939.

[17] Morse, P. M. and Feshbach, H., *Methods of Theoretical Physics, Part I.* McGraw-Hill, 1953.

[18] Reisner, S., "Random polytopes and the volume-product of symmetric convex bodies," *Math. Scand.*, vol. 57, pp. 386–392, 1985.

[19] Reisner, S., "Zonoids with minimal volume-product," *Math. Z.*, vol. 192, pp. 339–346, 1986.

[20] Reisner, S., "Minimal volume product in banach spaces with a 1-unconditional basis," *Journal of the London Mathematical Society (2)*, vol. 36, pp. 126–136, 1987.

[21] Rockafellar, R. T., *Convex Analysis.* Princeton University Press, 1970.

[22] Saint-Raymond, J., "Sur le volume des corps convexes symetriques," 1980/1981.

[23] Santalo, L. A., "Un invariante afin para los cuerpos convexos des espacio de n dimensionaes," *Portugaliae Math.*, vol. 8, pp. 155–161, 1949.

[24] Schneider, R., *Convex Bodies: The Brunn-Minkowski Theory.* Cambridge University Press, 1993.

[25] Stancu, A., "Two volume produc inequalities and their applications," *Canad. Math. Bull.*, vol. 52, pp. 464–472, 2009.

[26] Tao, T., *Open question: the Mahler conjecture on convex bodies.* Department of Mathematics, University of Los Angeles. The article is out of Tao's blog and available including all comments at http://terrytao.wordpress.com/2007/03/08/open-problem-the-mahler-conjecture-on-convex-bodies/ - March 2010.

[27] Tao, T., *Santalo's Inequality.* Department of Mathematics, University of Los Angeles. The article was originally intended for Terence Tao's book "Structure and Randomness: pages from year one of a mathematical blog" but got cut off. It is available at http://www.math.ucla.edu/∼tao/preprints/Expository/santalo.dvi - March 2010.

[28] Webster, R., *Convexity.* Oxford University Press, 1994.

[29] White, E., *Polar - Legendre Duality in Convex Geometry and geometric flows.* Georgia Institute of Technology. Master Thesis in Mathematics.

[30] Wolfram Research, I., *Mathematica Edition: Version 7.0*, 2008.